



# Variance-reduced estimation of Third-order statistics using control variates with splitting

Cristóbal H. Acevedo <sup>a</sup>, Marcos A. Valdebenito <sup>a</sup> , Iván V. González <sup>b</sup> , Héctor A. Jensen <sup>c</sup>, Matthias G.R. Faes <sup>a,d</sup>

<sup>a</sup> Chair for Reliability Engineering, TU Dortmund University, Leonhard-Euler-Strasse 5, 44227 Dortmund, Germany

<sup>b</sup> Department of Operational Intelligence, Esval, Valparaíso, Chile

<sup>c</sup> Universidad Técnica Federico Santa María, Dept. de Obras Civiles, Av. España 1680, Valparaíso, Chile

<sup>d</sup> International Joint Research Center for Engineering Reliability and Stochastic Mechanics, Tongji University, Shanghai, China

## ARTICLE INFO

### Keywords:

Uncertainty quantification  
Third-order statistics  
Low-fidelity models  
Control Variates  
Splitting

## ABSTRACT

This work proposes an approach to improve the estimation accuracy and precision of the first three statistical moments of the response of uncertain systems by leveraging one or more low-fidelity models via Control Variates. The two main contributions are: (1) the derivation of explicit expressions for estimating the mean, variance, and third central moment; and (2) the incorporation of a Splitting technique that enables unbiased estimation of all sought moments. Compared to standard Monte Carlo simulation, the proposed method achieves the same precision with significantly fewer high-fidelity model evaluations, thus reducing the computational cost. The application of the proposed approach is also illustrated when dealing with high-dimensional problems.

## 1. Introduction

Numerical models allow to characterize the behavior of a physical system [1]. Thus, it is possible to analyze responses of interest of that system under different conditions. In such a context, it is of particular interest to analyze such responses whenever the input parameters of a numerical model are uncertain [2]. Indeed, in several practical cases, such input parameters cannot be identified in a crisp manner and then, their uncertainty should be reflected using an appropriate means such as, e.g. probability theory [3]. In that way, input parameters of a model are characterized as random variables (or random fields and/or stochastic processes in case of space/time dependence, see e.g. [4]). The latter means that the responses of interest also become uncertain and their uncertainty must be properly quantified in terms of probabilistic descriptors. Classical examples of such probabilistic descriptors comprise second-order statistics [5], probability distributions [6] or probabilities of exceedance [7], to name a few. In general, the calculation of these probabilistic descriptors is not a straightforward task and therefore, several specialized approaches for uncertainty propagation have been developed, including, for example, analytic methods [8,9], approximations [10,11], density evolution methods [12–14], surrogate modeling [15–17], advanced simulation approaches [18,19], etc. Although the aforementioned list is far from complete, it attests that the

development of approaches for uncertainty propagation is a topic of active research.

Several approaches for uncertainty propagation demand performing repeated simulations of the numerical model associated with a system for different realizations of the uncertain input parameters. This task can become quite demanding from a numerical viewpoint, particularly for those cases where evaluation of the numerical model entails considerable numerical effort. In this context, the model that provides the most accurate representation of the system is referred to as the *high-fidelity* (HF) model. To reduce computational costs, it is common to incorporate one or more *low-fidelity* (LF) models, that offer approximations of the HF model and whose evaluation is numerically less demanding than that of the HF model. There are different ways to construct LF models such as surrogate models, reduced order models (ROMs) or coarse discretizations [20–24]. The application of numerical models that possess different levels of fidelity for uncertainty propagation has been investigated in several contributions, for example surrogate-based Gaussian-process and co-kriging models [25–27], polynomial chaos expansions with bi- or multi-fidelity corrections [28–30], multifidelity importance sampling [31–33], and neural-network-based multifidelity surrogates [34,35]. Within this broad landscape, particular emphasis has been placed on the estimation of statistical moments

\* Corresponding author.

E-mail address: [marcos.valdebenito@tu-dortmund.de](mailto:marcos.valdebenito@tu-dortmund.de) (M.A. Valdebenito).

<https://doi.org/10.1016/j.ress.2025.111859>

Received 3 July 2024; Received in revised form 14 October 2025; Accepted 26 October 2025

Available online 29 October 2025

0951-8320/© 2025 The Authors. Published by Elsevier Ltd. This is an open access article under the CC BY license (<http://creativecommons.org/licenses/by/4.0/>).

of the response. Those methods include multilevel Monte Carlo (MLMC) methods [36–40], multifidelity Monte Carlo (MFMC) methods [41–45], multilevel best linear unbiased estimator (MLBLUE) approach [46,47], and multilevel-multifidelity (MLMF) approaches [48–51]. Within this framework, the aim of this manuscript lies precisely on the issue of uncertainty propagation when dealing with both a high-fidelity and one or more low-fidelity models. More specifically, the probabilistic descriptors of interest are the first three moments (mean, variance, and third central moment) of a response of interest of an engineering system and the objective is to estimate these statistics with high precision (that is, with low variance) and reduced numerical efforts. The class of problems considered in this contribution includes both linear static systems and nonlinear dynamic systems. Uncertainty is propagated by means of Monte Carlo simulation (MCS) and Control Variates, see e.g. [52–54]. The Control Variates approach allows aggregating numerical simulations conducted using the HF and LF models, such that all three moments of the response can be estimated with reduced variance, even in cases where the statistics associated with the LF models are not known in closed form and must be obtained via simulation [55]. When compared with the literature, this work offers two important contributions. First, explicit expressions for estimating the first three moments of the response (mean, variance, and third central moment), as well as the variances of these estimators, are provided. While the estimation of the mean is standard in the literature, and some contributions address the variance (see, e.g., [56–58]), to the best knowledge of the authors, the third central moment has not been previously considered in this context. Consideration of the first three moments is very relevant, as information on the third moment can reveal the extent of non-Gaussianity of an uncertain response. Such information can provide valuable insight, as considering second-order statistics alone may neglect, e.g. asymmetry or tail distribution effects [59]. Second, the calculation of the control parameters associated with the application of Control Variates is addressed using a technique known as Splitting [60]. Such a technique plays a key role, as its application allows calculating unbiased estimators of the first- and higher-order statistics while still considering the same set of samples for estimating both the statistics and the so-called control parameters, which are key ingredients within the Control Variates framework. In addition, the proposed methodology is demonstrated in applications involving high-dimensional random input spaces, which is not commonly addressed in the context of variance reduction with multifidelity estimators.

This work is organized in the following way. Section 2 formulates the problem under consideration as well as the basic tools for analysis, namely Monte Carlo simulation. Section 3 focuses on the deduction of estimators of the first three moments of the response within the framework of Control Variates, with emphasis on the reduction of the variance of those estimators as well as avoiding bias through Splitting. Section 4 illustrates the application of the proposed framework to a test case and two examples, including both linear static and nonlinear dynamic systems. Conclusions and outlook for future work are discussed in Section 5.

## 2. Problem formulation

### 2.1. System characterization and response of interest

The class of problems considered in this work involves physical systems whose behavior depends on uncertain input parameters. These systems may be static or dynamic, linear or nonlinear. Let  $\theta \in \mathbb{R}^{n_\theta \times 1}$  denote a vector of uncertain input parameters, whose joint probability density function is denoted as  $p_\theta(\theta)$ . These parameters may represent, for example, material properties or loading parameters. The computational model, denoted as  $\mathcal{M}(\theta)$ , produces a system response based on a realization of the input vector  $\theta$ . The output of the model  $\mathcal{M}(\theta)$  may be high-dimensional (e.g., a time history). Nevertheless, it is assumed

that the response of interest  $r(\theta)$  can be extracted as a scalar functional of the model response. The response of interest is thus defined as:

$$r(\theta) = Q(\mathcal{M}(\theta)), \quad (1)$$

where  $Q(\cdot)$  denotes a functional that maps the model output to a real scalar value. In the following, it is assumed that this response  $r(\theta)$  corresponds to the so-called high-fidelity (HF) model.

As  $\theta$  is a random vector, the response of interest  $r(\theta)$  becomes a random variable. The objective of this work is to quantify the uncertainty of this response in terms of its first three moments, namely:

- The mean (first raw moment):  $\mu'_1 = \mathbb{E}[r]$  (where  $\mathbb{E}[\cdot]$  denotes expectation),
- The variance (second central moment):  $\mu_2 = \mathbb{E}[(r - \mu'_1)^2]$ ,
- The third central moment:  $\mu_3 = \mathbb{E}[(r - \mu'_1)^3]$ .

### 2.2. Monte Carlo simulation

The implicit dependence of the response of interest  $r$  with respect to the uncertain input parameters  $\theta$  of a model prevents calculating its first three moments analytically in practical situations. In such case, Monte Carlo simulation (see, e.g. [61]) offers a feasible means for estimating these moments. For such purpose,  $n$  independent, identically distributed realizations of the random variable vector  $\theta$  are generated and collected in matrix  $\theta_n$ , where the  $i$ th realization is denoted as  $\theta_{n,i}$ . Then, unbiased estimators for mean and variance are [61]:

$$\widehat{\mu}'_1(r; \theta_n) = \frac{1}{n} \sum_{i=1}^n r(\theta_{n,i}), \quad (2)$$

$$\widehat{\mu}_2(r; \theta_n) = \frac{1}{n-1} \sum_{i=1}^n \left( r(\theta_{n,i}) - \frac{1}{n} \sum_{j=1}^n r(\theta_{n,j}) \right)^2, \quad (3)$$

$$\widehat{\mu}_3(r; \theta_n) = \frac{2 \left( \sum_{i=1}^n r(\theta_{n,i}) \right)^3 - 3n \left( \sum_{i=1}^n r(\theta_{n,i}) \right) \left( \sum_{i=1}^n r^2(\theta_{n,i}) \right) + n^2 \left( \sum_{i=1}^n r^3(\theta_{n,i}) \right)}{(n-2)(n-1)n}, \quad (4)$$

where  $\widehat{(\cdot)}$  denotes an estimator of a quantity. The variance  $\widehat{\sigma}^2$  of each of these estimators is [3]:

$$\widehat{\sigma}^2 \left[ \widehat{\mu}'_1(r; \theta_n) \right] = \frac{\widehat{\mu}_2(r; \theta_n)}{n}, \quad (5)$$

$$\widehat{\sigma}^2 \left[ \widehat{\mu}_2(r; \theta_n) \right] = \frac{\widehat{\mu}_4(r; \theta_n)}{n} - \frac{(n-3) \widehat{\mu}_2^2(r; \theta_n)}{(n-1)n}, \quad (6)$$

$$\begin{aligned} \widehat{\sigma}^2 \left[ \widehat{\mu}_3(r; \theta_n) \right] &= \frac{3(20-12n+3n^2)}{(n-2)(n-1)n} \widehat{\mu}_2^3(r; \theta_n) - \frac{(n-10)}{(n-1)n} \widehat{\mu}_3^2(r; \theta_n) \\ &\quad - \frac{3(2n-5)}{(n-1)n} \widehat{\mu}_2 \widehat{\mu}_4(r; \theta_n) + \frac{1}{n} \widehat{\mu}_6(r; \theta_n), \end{aligned} \quad (7)$$

where  $\widehat{\mu}_4(r; \theta_n)$  and  $\widehat{\mu}_6(r; \theta_n)$  are the estimates of the fourth- and sixth-order central moments of the response  $r$ , respectively. Formulas for calculating  $\widehat{\mu}_4(r; \theta_n)$ ,  $\widehat{\mu}_2^2(r; \theta_n)$ ,  $\widehat{\mu}_6(r; \theta_n)$ ,  $\widehat{\mu}_3^2(r; \theta_n)$ ,  $\widehat{\mu}_2^3(r; \theta_n)$ , and  $\widehat{\mu}_2 \widehat{\mu}_4(r; \theta_n)$  can be found in Appendix A in Eqs. (A.7), (A.9), (A.12), (A.14), (A.15), and (A.17), respectively, where one needs to consider  $q = 0$ . In principle, the variances of the estimators for the mean, variance and third central moment as shown in Eqs. (5), (6) and (7) are related with the level of precision of the estimates. Naturally, the precision can be improved by decreasing the variance, which in turn demands increasing the number of samples  $n$ . However, this can entail significant numerical efforts due to the repeated evaluation of the HF model. An alternative would be to consider one or more low-fidelity (LF) models whose numerical evaluations are less demanding than that of the HF model. However, the challenge in such situation would be how to leverage multiple LF models and still get the first three moments of the response associated with the HF model. Such challenge is addressed in detail in Section 3.

As a side remark, it is important to mention that at this stage, it is assumed that the LF models are already available, as the construction of such models is not the main focus of this work. Nevertheless and for completeness, details about the construction of the LF models are discussed for the specific examples considered in this work (see Section 4).

### 3. Variance-reduced estimators of first-, second-, and third-order statistics using control variates with splitting

#### 3.1. General remarks

This Section discusses the integration of the high-fidelity (HF) model along with one or more low-fidelity (LF) models for estimating the first three moments of the response of an uncertain model. Section 3.2 discusses the estimation of the mean, where Section 3.2.1 focuses on the application of Control Variates while Section 3.2.2 shows the Splitting scheme. Then, the estimation of the second and third central moments is discussed in Sections 3.3 and 3.4, respectively. Section 3.5 discusses the number of evaluations to be carried out for the HF model and the LF models, while Section 3.6 discusses some practical implementation issues.

Before discussing the details on the application of Control Variates with Splitting, some definitions used in this paper are provided.

*High- and low-fidelity models.* We denote by  $r$  the response of the high-fidelity (HF) model, and by  $\tilde{r}_\ell$  the response of the  $\ell$ th low-fidelity (LF) model. For convenience, the LF responses are collected in the vector

$$\tilde{\mathbf{r}} = [\tilde{r}_1, \tilde{r}_2, \dots, \tilde{r}_L]^\top, \quad (8)$$

where  $L$  denotes the number of LF models considered, and  $(\cdot)^\top$  indicates the transpose of the argument.

*Moments and co-moments.* For a single model response  $y$ , the central moment of order  $p$  is defined as

$$\mu_p(y) := \mathbb{E}[(y - \mathbb{E}[y])^p], \quad (9)$$

where  $\mathbb{E}[\cdot]$  denotes expectation of the argument. For two model responses  $y_a$  and  $y_b$ , the bivariate central co-moment of order  $(p, q)$  is defined as

$$\mu_{p,q}(y_a, y_b) := \mathbb{E}[(y_a - \mathbb{E}[y_a])^p (y_b - \mathbb{E}[y_b])^q]. \quad (10)$$

Here,  $y$ ,  $y_a$ , and  $y_b$  may represent either the HF response  $r$  or any LF response  $\tilde{r}_\ell$  defined in the previous section. Explicit unbiased estimators for the required moments and co-moments are provided in Appendix A.

*Sample sets.* To estimate the statistical moments introduced in the previous section, model responses must be evaluated on suitable sample sets. The notation for the sample sets considered to evaluate the HF and LF models is defined as follows:

$$\Theta_n := \{\theta_{n,i}\}_{i=1}^n, \quad (11)$$

$$\Theta_m := \{\theta_{m_1}, \theta_{m_2}, \dots, \theta_{m_L}\}, \quad (12)$$

$$\Theta_{m_\ell} := \{\theta_{m_\ell,i}\}_{i=1}^{m_\ell}, \quad \ell = 1, \dots, L. \quad (13)$$

The set  $\Theta_n$  represents the shared sample set of size  $n$ , which is used by both the HF model  $r$  and all LF models  $\tilde{r}_\ell$ . On the other hand,  $\Theta_m$  represents the collection of sample sets  $\Theta_{m_\ell}$ ,  $\ell = 1, \dots, L$ , each associated with the low-fidelity model  $\tilde{r}_\ell$ . Each set  $\Theta_{m_\ell}$  contains  $m_\ell$  samples of  $\Theta$ , used exclusively for evaluating the corresponding LF model  $\tilde{r}_\ell$ . The sets  $\Theta_{m_\ell}$  are mutually independent and also independent of  $\Theta_n$ . The sample sizes  $m_\ell$  may differ across LF models. In practical applications, it is usually verified that  $m_\ell \gg n$  for  $\ell = 1, \dots, L$ , since evaluations of the LF models are typically much cheaper than those of the HF model.

*Moment estimators for HF and LF models.* For the high-fidelity (HF) model response  $r$ , the estimator of a generic moment  $\mu$  based on the shared sample set  $\Theta_n$  is defined as  $\hat{\mu}(r; \Theta_n)$ .

Based on the vector of LF responses  $\tilde{\mathbf{r}}$  introduced in (8), we compactly define the corresponding estimators of the same generic moment  $\mu$  as

$$\hat{\mu}(\tilde{\mathbf{r}}; \Theta_n) = [\hat{\mu}(\tilde{r}_1; \Theta_n), \hat{\mu}(\tilde{r}_2; \Theta_n), \dots, \hat{\mu}(\tilde{r}_L; \Theta_n)]^\top, \quad (14)$$

$$\hat{\mu}(\tilde{\mathbf{r}}; \Theta_m) = [\hat{\mu}(\tilde{r}_1; \Theta_{m_1}), \hat{\mu}(\tilde{r}_2; \Theta_{m_2}), \dots, \hat{\mu}(\tilde{r}_L; \Theta_{m_L})]^\top. \quad (15)$$

Here,  $\mu$  generically denotes any of the first three moments considered in this work; that is,  $\mu_1$  (mean),  $\mu_2$  (variance), or  $\mu_3$  (third central moment). In this way,  $\hat{\mu}(r; \cdot)$  denotes the HF estimate of the selected moment, while  $\hat{\mu}(\tilde{r}_\ell; \cdot)$  denotes the LF estimate for the  $\ell$ th LF model. Both HF and LF estimates are computed with the corresponding single-model formula: Eq. (2) if  $\mu = \mu_1$ , Eq. (3) if  $\mu = \mu_2$ , and Eq. (4) if  $\mu = \mu_3$ . Estimates evaluated on  $\Theta_n$  use the shared sample set, whereas those on  $\Theta_{m_\ell}$ ,  $\ell = 1, \dots, L$ , use the independent LF sets (see Eqs. (11)–(13)).

These notations will be used repeatedly in Sections 3.2–3.4.

#### 3.2. Estimation of the mean

##### 3.2.1. Application of control variates

The estimate of the mean  $\mu_1'(r)$  according to Control Variates is the following (see, e.g. [55,61]).

$$\hat{\mu}_1'^{\text{CV}}(r, \tilde{\mathbf{r}}; \Theta_n, \Theta_m) = \hat{\mu}_1'(r; \Theta_n) - \alpha^\top [\hat{\mu}_1'(\tilde{\mathbf{r}}; \Theta_n) - \hat{\mu}_1'(\tilde{\mathbf{r}}; \Theta_m)]. \quad (16)$$

Here,  $\hat{\mu}_1'(r; \Theta_n)$  denotes the HF mean estimator computed on the shared sample set  $\Theta_n$ . The terms  $\hat{\mu}_1'(\tilde{\mathbf{r}}; \Theta_n)$  and  $\hat{\mu}_1'(\tilde{\mathbf{r}}; \Theta_m)$  are the corresponding vectors of LF estimators, obtained as particular cases of the generic definitions in Eqs. (14)–(15) with  $\mu = \mu_1'$ . Additionally, the vector  $\alpha$  denotes the *control parameters* associated with Control Variates, whose calculation is discussed later in this work.

To better understand the rationale behind Eq. (16), its structure can be clarified by analyzing its main components: the term  $\alpha^\top \hat{\mu}_1'(\tilde{\mathbf{r}}; \Theta_m)$  is a linear combination of low-fidelity (LF) mean estimators. Because it relies on the LF models, it is not accurate with respect to the HF mean, but it is inexpensive to evaluate (it only involves LF models). Then, the term  $\hat{\mu}_1'(r; \Theta_n) - \alpha^\top \hat{\mu}_1'(\tilde{\mathbf{r}}; \Theta_n)$  acts as a correction, subtracting a linear combination of LF based estimators (computed on the shared samples) and adding the HF estimate. This correction is usually cheap (it requires only  $n$  HF evaluations) and exhibits low variability whenever the HF and LF models are strongly correlated.

In summary, the estimator in Eq. (16) combines evaluations from both LF and HF models:

- *Low-fidelity (LF) models:* a total of  $nL + \sum_{\ell=1}^L m_\ell$  evaluations, including both the  $n$  shared evaluations and the additional  $m_\ell$  evaluations for each LF model.
- *High-fidelity (HF) model:* only  $n$  evaluations, corresponding to the shared sample set  $\Theta_n$ .

Together, these evaluations produce an estimate of the mean  $\hat{\mu}_1'^{\text{CV}}(r, \tilde{\mathbf{r}}; \Theta_n, \Theta_m)$ .

To determine the value of the optimal control parameters  $\alpha$ , it is noted that these parameters are real numbers selected in such a way that the variance of the estimator in Eq. (16) is minimized. For this reason, it is useful to calculate this variance, denoted by  $\sigma^2[\cdot]$ , which is equal to the following expression (see, e.g., [55,60,61]):

$$\begin{aligned} \sigma^2 \left[ \hat{\mu}_1'^{\text{CV}}(r, \tilde{\mathbf{r}}; \Theta_n, \Theta_m) \right] &= A_1(r; \Theta_n) \\ &\quad - 2\alpha^\top A_2(r, \tilde{\mathbf{r}}; \Theta_n) \\ &\quad + \alpha^\top \left( A_3(\tilde{\mathbf{r}}; \Theta_n) + A_4(\tilde{\mathbf{r}}; \Theta_m) \right) \alpha. \end{aligned} \quad (17)$$

In Eq. (17), the terms  $A_1$ ,  $A_2$ ,  $A_3$ , and  $A_4$  correspond to the variance and covariance contributions associated with the HF and LF estimators of the mean. Specifically,  $A_1(r; \Theta_n)$  denotes the variance of the HF estimator of the mean,  $A_2(r, \tilde{r}; \Theta_n)$  is the vector of covariances between the HF estimator and each LF estimator computed with the shared sample set  $\Theta_n$ ,  $A_3(\tilde{r}; \Theta_n)$  is the covariance matrix among LF estimators based on the shared samples, and  $A_4(\tilde{r}; \Theta_m)$  is the diagonal covariance matrix containing the variances of the LF estimators obtained from the independent sample sets  $\Theta_{m_\ell}$ ,  $\ell = 1, \dots, L$ . Their explicit definitions are provided in Appendix B.1.

It is observed from Eq. (17) that the variance of the Control Variates estimate of the mean is a quadratic function with respect to the vector of control parameters  $\alpha$ . Therefore, it is possible to select such parameter vector such that the variance of the estimator of the mean is minimized, leading to the following equation for selecting the optimal control parameters  $\alpha^*$  (see, e.g. [55,61]):

$$\alpha^* = \left( A_3(\tilde{r}; \Theta_n) + A_4(\tilde{r}; \Theta_m) \right)^{-1} A_2(r, \tilde{r}; \Theta_n). \quad (18)$$

Inserting these optimal control parameters  $\alpha^*$  in Eq. (17) yields the minimum possible variance for the estimator of the mean, that is (see, e.g. [55,61]):

$$\hat{\sigma}^2 \left[ \hat{\mu}_1^{\text{CV}}(r, \tilde{r}; \Theta_n, \Theta_m) \right] \Big|_{\alpha=\alpha^*} = A_1(r; \Theta_n) - A_2(r, \tilde{r}; \Theta_n)^T \left( A_3(\tilde{r}; \Theta_n) + A_4(\tilde{r}; \Theta_m) \right)^{-1} A_2(r, \tilde{r}; \Theta_n). \quad (19)$$

Eq. (19) reveals that the variance of the estimator of the mean calculated with Control Variates is actually equal to the variance that would be associated with Monte Carlo simulation of the HF model (represented in the term  $A_1(r; \Theta_n)$ , see also Eq. (5)) minus a term which depends on the covariances between the response of the HF model and those of the LF models (represented by  $A_2(r, \tilde{r}; \Theta_n)$ ). To understand the structure of Eq. (19), it is useful to consider two extreme cases. In the worst-case scenario where there is no covariance between the HF model and the LF models, the vector of covariances vanishes, i.e.  $A_2(r, \tilde{r}; \Theta_n) = \mathbf{0}$ , and the variance of the estimator of the mean reduces to that of Monte Carlo simulation using the HF model only. In the best-case scenario where the LF models provide high quality approximations of the HF model, it is expected that the corresponding covariance terms dominate and the variance of the estimator in Eq. (19) becomes very small whenever the additional sample sizes  $m_\ell$ ,  $\ell = 1, \dots, L$ , are relatively large. In other words, in this best-case scenario, the LF models could be regarded as being as good as the HF model. In practical applications, one may expect that the ability of the LF models for approximating the HF model will lie in between the two extreme cases described above. In fact, if the worst-case scenario occurs, it implies that all LF models are of extremely low quality and in such case, it is not possible to leverage them. On the contrary, if the LF models are as good as the HF model, that would most likely imply that numerical costs associated with the evaluation of these LF models are close to those of the HF model, which would bring no major benefits.

### 3.2.2. Application of control variates with splitting

Control Variates provides the framework to estimate the mean response of the HF model by employing both the HF and LF models, as noted from Eq. (16). The variance of this estimator is minimal (see Eq. (19)) if one considers the optimal control parameters (see Eq. (18)). However, this framework will produce estimates which are *biased*, as discussed in detail in [52]. The reason for this undesirable behavior is that the optimal control parameters in Eq. (18) are calculated with the very same set of samples of  $r$  and  $\tilde{r}$  (from the HF and LF models, respectively) that are used to estimate the mean in Eq. (16). In fact, the effect of bias could be particularly notorious in case that the number of samples  $n$  of the response  $r$  (calculated with the HF model) is small, which is usually the case (because the HF model is numerically expensive to evaluate). A formal proof of how this bias arises is provided

**Table 1**

Subset identifier  $j$  and subset controller  $\tau(j)$ .

$j$ (subset identifier)	$\tau(j)$ (subset controller)
1	2
2	3
3	1

in Appendix C. A workaround that would eliminate the effect of bias would be to generate a new set of samples of the response  $r$  and  $\tilde{r}$  to calculate the control parameters  $\alpha$ . Such a strategy has been used in the past in the context of Control Variates [52] and multifidelity Monte Carlo [41,42]. However, such an alternative would entail additional evaluations of the HF model, which is undesirable because it would increase numerical costs. A strategy that does eliminate bias and which does not demand additional evaluations of the high-fidelity (HF) model is the so-called *Splitting*. In essence, Splitting means separating the set of available samples of the response  $r$  and  $\tilde{r}$  into subsets and then, calculate the optimal control parameters and the sought statistics at the level of those subsets, and then finally aggregate the results from those subsets. In particular, the Splitting considered here is the one proposed in [60], which has been shown to produce unbiased estimates of the sought statistics. In this work, the Splitting technique is applied for the specific case of three subsets of samples, as this is the minimum possible number of subsets that must be considered in order to eliminate the effect of bias in the estimators of the sought statistics. While in principle it is possible to consider a larger number of subsets, this would increase the variance of the estimated quantities, as shown in [60]. Therefore, in the following, the details of this specific Splitting technique are discussed considering only three subsets of samples.

Assume that the sizes  $n$  and  $m_\ell$ ,  $\ell = 1, \dots, L$ , of the sample sets  $\Theta_n$  and  $\Theta_{m_\ell}$ , defined in Eqs. (11)–(13), are selected such that they are all multiple of 3. Then, the shared sample set  $\Theta_n$  and each independent LF sample set  $\Theta_{m_\ell}$  are split into three subsets, each of them with  $n^* = n/3$  and  $m_\ell^* = m_\ell/3$  samples, respectively. These subsets are denoted as  $\Theta_{n^*,j}$  and  $\Theta_{m_\ell^*,j}$ , where  $j$  is an integer denoting the subset number such that  $j \in \{1, 2, 3\}$ . These subsets of samples are composed as follows.

$$\Theta_{n^*,j} = [\theta_{n, (1+(j-1)n^*)}, \dots, \theta_{n, (n^*+(j-1)n^*)}], \quad j = 1, 2, 3, \quad (20)$$

$$\Theta_{m_\ell^*,j} = [\theta_{m_\ell, (1+(j-1)m_\ell^*)}, \dots, \theta_{m_\ell, (m_\ell^*+(j-1)m_\ell^*)}], \quad j = 1, 2, 3. \quad (21)$$

Moreover, consider the integer variable  $\tau(j)$  which is denoted as a *subset controller* and is defined as shown in Table 1.

With the above definitions, the estimate for the mean of the response  $r$  that considers samples of the HF and LF models by means of Control Variates and which includes the Splitting scheme is the following:

$$\hat{\mu}_1^{\text{CV+S}}(r, \tilde{r}; \Theta_n, \Theta_m) = \frac{1}{3} \sum_{j=1}^3 \hat{\mu}_1^{\text{CV},(j)}(r, \tilde{r}; \Theta_{n^*,j}, \Theta_{m^*,j}). \quad (22)$$

In the above equation,  $\hat{\mu}_1^{\text{CV},(j)}$  denotes the  $j$ th Control Variates estimate of the mean of the response, which is calculated as:

$$\begin{aligned} \hat{\mu}_1^{\text{CV},(j)}(r, \tilde{r}; \Theta_{n^*,j}, \Theta_{m^*,j}) &= \hat{\mu}_1^*(r; \Theta_{n^*,j}) - \alpha_{\tau(j)}^*{}^T \hat{\mu}_1^*(\tilde{r}; \Theta_{n^*,j}) \\ &\quad + \alpha_{\tau(j)}^*{}^T \hat{\mu}_1^*(\tilde{r}; \Theta_{m^*,j}), \quad j = 1, 2, 3. \end{aligned} \quad (23)$$

where the optimal control parameters  $\alpha_{\tau(j)}^*$  are defined as:

$$\alpha_{\tau(j)}^* = \left( A_3(\tilde{r}; \Theta_{n^*,\tau(j)}) + A_4(\tilde{r}; \Theta_{m^*,\tau(j)}) \right)^{-1} A_2(r, \tilde{r}; \Theta_{n^*,\tau(j)}), \quad j = 1, 2, 3. \quad (24)$$

A close examination of Eqs. (22), (23) and (24) allows to understand the characteristics of the estimator for the mean including both Control Variates and Splitting. Eq. (22) is nothing but an average of the three estimates of the mean produced with Control Variates as



shown in Eq. (23). However, the estimator in Eq. (23) has a very special structure. Indeed, the means  $\mu'_1$  involved in this equation are calculated with the sample subsets  $\Theta_{n^*,j}$  and  $\Theta_{m^*,j}$  while the optimal control parameters  $\alpha_{\tau(j)}^*$  (which are defined in Eq. (24)) are calculated with the sample subsets  $\Theta_{n^*,\tau(j)}$  and  $\Theta_{m^*,\tau(j)}$ . It is readily seen from Table 1 that  $j \neq \tau(j)$ ,  $j = 1, 2, 3$ . This implies that when  $\hat{\mu}_1^{CV(j)}$  is calculated, the sample subsets used for estimating the optimal control parameters are always different from those used to calculate the means involved in the estimator. Such characteristic effectively eliminates the effect of bias from the estimator (see Appendix C for the proof that this technique produces unbiased estimators).

The variance of the estimator in Eq. (22) can be calculated by means of (see [60]):

$$\hat{\sigma}^2 \left[ \hat{\mu}_1^{CV+S}(r, \tilde{r}; \Theta_n, \Theta_m) \right] = \frac{1}{3^2} \sum_{j=1}^3 \hat{\sigma}^2 \left[ \hat{\mu}_1^{CV(j)}(r, \tilde{r}; \Theta_{n^*,j}, \Theta_{m^*,j}) \right], \quad (25)$$

where the variance of  $\hat{\mu}_1^{CV(j)}$  is:

$$\begin{aligned} \hat{\sigma}^2 \left[ \hat{\mu}_1^{CV(j)}(r, \tilde{r}; \Theta_{n^*,j}, \Theta_{m^*,j}) \right] &= A_1(r; \Theta_{n^*,j}) - 2 \alpha_{\tau(j)}^{*\top} A_2(r, \tilde{r}; \Theta_{n^*,j}) \\ &+ \alpha_{\tau(j)}^{*\top} \left( A_3(\tilde{r}; \Theta_{n^*,j}) + A_4(\tilde{r}; \Theta_{m^*,j}) \right) \alpha_{\tau(j)}^*, \quad j = 1, 2, 3. \end{aligned} \quad (26)$$

While the above expressions for the estimator of the mean and its variance using Control Variates with Splitting are rather lengthy, it should be noted that they are actually quite similar to those involving Control Variates only, except for the fact that one needs to keep track of different quantities at the subset level. This does not demand significant additional efforts. The latter is particularly true given the fact that no additional evaluations of the high-fidelity (HF) model are required for implementing Control Variates with Splitting.

### 3.3. Estimation of the variance

Section 3.2 has focused on the estimation of the mean of the response of interest  $r$  and the variance of that estimator. In here, the focus is on the calculation of the variance of the response of interest and the variance of that estimator. To estimate the variance of  $r$ , Control Variates and Splitting are immediately adopted, producing expressions similar to those for estimating the mean as shown in Eqs. (22) and (23). As demonstrated in Appendix C, the adoption of Splitting produces unbiased estimators. This leads to the following estimator for the variance:

$$\hat{\mu}_2^{CV+S}(r, \tilde{r}; \Theta_n, \Theta_m) = \frac{1}{3} \sum_{j=1}^3 \hat{\mu}_2^{CV(j)}(r, \tilde{r}; \Theta_{n^*,j}, \Theta_{m^*,j}), \quad (27)$$

where  $\hat{\mu}_2^{CV(j)}$  denotes the  $j$ th Control Variates estimate of the variance of the response, which is calculated as:

$$\begin{aligned} \hat{\mu}_2^{CV(j)}(r, \tilde{r}; \Theta_{n^*,j}, \Theta_{m^*,j}) &= \hat{\mu}_2(r; \Theta_{n^*,j}) - \gamma_{\tau(j)}^\top \hat{\mu}_2(\tilde{r}; \Theta_{n^*,j}) \\ &+ \gamma_{\tau(j)}^\top \hat{\mu}_2(\tilde{r}; \Theta_{m^*,j}), \quad j = 1, 2, 3. \end{aligned} \quad (28)$$

Here,  $\hat{\mu}_2(r; \Theta_{n^*,j})$  denotes the HF variance estimator of the second central moment computed by means of Eq. (3). The terms  $\hat{\mu}_2(\tilde{r}; \Theta_{n^*,j})$  and  $\hat{\mu}_2(\tilde{r}; \Theta_{m^*,j})$  are the corresponding vectors of LF variance estimators, obtained as particular cases of the generic definitions in Eqs. (14)–(15) with  $\mu = \mu_2$ . Moreover,  $\gamma_{\tau(j)}$  denotes the vector of control parameters for estimating the variance of the response.

The variance of the estimator in Eq. (27) is given by the summation of the variances of the terms of the associated summation, that is:

$$\hat{\sigma}^2 \left[ \hat{\mu}_2^{CV+S}(r, \tilde{r}; \Theta_n, \Theta_m) \right] = \frac{1}{3^2} \sum_{j=1}^3 \hat{\sigma}^2 \left[ \hat{\mu}_2^{CV(j)}(r, \tilde{r}; \Theta_{n^*,j}, \Theta_{m^*,j}) \right], \quad (29)$$

where the variance term  $\hat{\sigma}^2 \left[ \hat{\mu}_2^{CV(j)} \right]$  is equal to:

$$\hat{\sigma}^2 \left[ \hat{\mu}_2^{CV(j)}(r, \tilde{r}; \Theta_{n^*,j}, \Theta_{m^*,j}) \right] = B_1(r; \Theta_{n^*,j}) - 2 \gamma_{\tau(j)}^\top B_2(r, \tilde{r}; \Theta_{n^*,j})$$

$$+ \gamma_{\tau(j)}^\top \left( B_3(\tilde{r}; \Theta_{n^*,j}) + B_4(\tilde{r}; \Theta_{m^*,j}) \right) \gamma_{\tau(j)}, \quad j = 1, 2, 3, \quad (30)$$

and where  $B_1$ ,  $B_2$ ,  $B_3$  and  $B_4$  correspond to the variance and covariance terms associated with the HF and LF estimators of the variance. Their explicit definitions are provided in Appendix B.2.

A comparison between Eqs. (26) and (30) indicates that they possess an overall similar structure, although Eq. (30) is more involved, as it comprises estimates of bivariate central co-moments up to the fourth order. Detailed expressions for evaluating all the estimates of bivariate co-moments can be found in Appendix A.

Eq. (30) allows calculating the variance of the variance estimator  $\hat{\mu}_2^{CV(j)}$ ,  $j = 1, 2, 3$ . As it is a quadratic function with respect to the control parameters  $\gamma_{\tau(j)}$ , it is possible to find the values of these control parameters such that the variance is minimized, leading to the following expression for the optimal control parameters  $\gamma_{\tau(j)}^*$ :

$$\gamma_{\tau(j)}^* = \left( B_3(\tilde{r}; \Theta_{n^*,\tau(j)}) + B_4(\tilde{r}; \Theta_{m^*,\tau(j)}) \right)^{-1} B_2(r, \tilde{r}; \Theta_{n^*,\tau(j)}), \quad j = 1, 2, 3. \quad (31)$$

Once the optimal values  $\gamma_{\tau(j)}^*$  of the control parameters have been determined, they can be used together with Eqs. (27) and (28) in order to determine the variance of the response. Moreover, the variance of the variance estimator can be calculated by considering these optimal control parameters  $\gamma_{\tau(j)}^*$  together with Eqs. (29) and (30). A detailed proof of the unbiasedness of the proposed estimator for the variance is provided in Appendix C.

### 3.4. Estimation of the third-order moment

As in the cases of the mean and the variance (see Sections 3.2 and 3.3), the estimation of the third central moment  $\mu_3(r)$  of the response of interest  $r$  is carried out using the Control Variates with Splitting approach. As demonstrated in Appendix C, such an approach produces unbiased estimators of the sought third-order central moment. The estimator is constructed by averaging three independent control variates estimators, each of them based on disjoint subsets of the original sample sets  $\Theta_n$  and  $\Theta_m$ . This leads to the following expression:

$$\hat{\mu}_3^{CV+S}(r, \tilde{r}; \Theta_n, \Theta_m) = \frac{1}{3} \sum_{j=1}^3 \hat{\mu}_3^{CV(j)}(r, \tilde{r}; \Theta_{n^*,j}, \Theta_{m^*,j}). \quad (32)$$

Each individual estimator  $\hat{\mu}_3^{CV(j)}$  is calculated as:

$$\begin{aligned} \hat{\mu}_3^{CV(j)}(r, \tilde{r}; \Theta_{n^*,j}, \Theta_{m^*,j}) &= \hat{\mu}_3(r; \Theta_{n^*,j}) - \eta_{\tau(j)}^\top \hat{\mu}_3(\tilde{r}; \Theta_{n^*,j}) \\ &+ \eta_{\tau(j)}^\top \hat{\mu}_3(\tilde{r}; \Theta_{m^*,j}), \quad j = 1, 2, 3. \end{aligned} \quad (33)$$

Here,  $\hat{\mu}_3(r; \Theta_{n^*,j})$  denotes the HF estimator of the third central moment computed by means of Eq. (4). The terms  $\hat{\mu}_3(\tilde{r}; \Theta_{n^*,j})$  and  $\hat{\mu}_3(\tilde{r}; \Theta_{m^*,j})$  are the corresponding vectors of LF estimators, obtained as particular cases of the generic definitions in Eqs. (14)–(15) with  $\mu = \mu_3$ . Moreover,  $\eta_{\tau(j)}$  denotes the vector of control parameters for estimating the third central moment of the response.

The variance of the estimator in Eq. (32) is computed as:

$$\hat{\sigma}^2 \left[ \hat{\mu}_3^{CV+S}(r, \tilde{r}; \Theta_n, \Theta_m) \right] = \frac{1}{3^2} \sum_{j=1}^3 \hat{\sigma}^2 \left[ \hat{\mu}_3^{CV(j)}(r, \tilde{r}; \Theta_{n^*,j}, \Theta_{m^*,j}) \right]. \quad (34)$$

Each term in the summation is computed as follows:

$$\begin{aligned} \hat{\sigma}^2 \left[ \hat{\mu}_3^{CV(j)}(r, \tilde{r}; \Theta_{n^*,j}, \Theta_{m^*,j}) \right] &= C_1(r; \Theta_{n^*,j}) - 2 \eta_{\tau(j)}^\top C_2(r, \tilde{r}; \Theta_{n^*,j}) \\ &+ \eta_{\tau(j)}^\top \left( C_3(\tilde{r}; \Theta_{n^*,j}) + C_4(\tilde{r}; \Theta_{m^*,j}) \right) \eta_{\tau(j)}, \quad j = 1, 2, 3, \end{aligned} \quad (35)$$

where the quantities  $C_1$ ,  $C_2$ ,  $C_3$  and  $C_4$  correspond to the variance and covariance terms associated with the HF and LF estimators of the third-order central moment. Their explicit definitions are provided in [Appendix B.3](#).

The optimal values of the control parameters  $\eta_{\tau(j)}^*$  are obtained by minimizing the variance in Eq. (35), leading to:

$$\eta_{\tau(j)}^* = \left( C_3(\tilde{r}; \Theta_{n^*, \tau(j)}) + C_4(\tilde{r}; \Theta_{m^*, \tau(j)}) \right)^{-1} C_2(r, \tilde{r}; \Theta_{n^*, \tau(j)}), \quad j = 1, 2, 3. \quad (36)$$

Once these optimal values have been determined, they can be substituted into Eqs. (33) and (35) to evaluate the third central moment and the variance of its estimator. A detailed proof of the unbiasedness of the proposed estimator for the third-order central moment is provided in [Appendix C](#).

### 3.5. Number of evaluations of the high- and low-fidelity models

The preceding discussion has assumed that the size  $n$  and the vector of sizes  $\mathbf{m}$  of the sample sets are already defined. Such an assumption is valid whenever the high- and low-fidelity (HF and LF) models have already been evaluated in the past, and when Control Variates is employed to aggregate the estimators to estimate the first- and higher-order statistics (e.g., up to the third central moment). However, in a more general setting, it may occur that no previous evaluations of the HF and LF models have been conducted and hence, it is necessary to select the sample sizes  $n$  and  $\mathbf{m}$  using a specific procedure. The approach considered in this contribution is to determine  $n$  and  $\mathbf{m}$  by solving an optimization problem that involves minimization of the numerical costs associated with the estimation of the first three moments of the response while ensuring a predefined level of precision. The precision is measured in terms of the coefficient of variation  $\delta$ , which is the standard deviation of the estimator divided by its expected value [61]. Such coefficient of variation must be below a predefined threshold level  $\delta_t$ , which can take values such as, e.g. 5% or 10%.

The practical implementation of the approach described in the preceding paragraph demands evaluating the mean and a standard deviation of an estimator for calculating its coefficient of variation. In principle, these quantities can be evaluated by applying Eqs. (22) and (25) for the mean, Eqs. (27) and (29) for the variance, and Eqs. (32) and (34) for the third moment. However, all of these quantities depend on co-moments (see [Appendix A](#)) which must be calculated with samples of the response from the HF and LF models. Therefore, the approach for estimating the sample sizes  $(n, \mathbf{m})$  must be applied iteratively. This implies that initial sample set sizes  $(n^{(0)}, \mathbf{m}^{(0)})$  are defined arbitrarily, then the corresponding samples of the HF and LF models are evaluated to estimate the co-moments and then, new values for the sample set sizes  $(n^{(1)}, \mathbf{m}^{(1)})$  are determined by optimization. In mathematical terms, a sequence of optimization problems needs to be solved. The  $k$ th ( $k \geq 1$ ) problem has the form:

$$(n^{(k)}, \mathbf{m}^{(k)}) = \arg \min_{(n, \mathbf{m})} n_{\text{eq}}, \quad (37)$$

subject to the following constraints:

$$n_{\text{eq}} = n + \sum_{\ell=1}^L (n + m_{\ell}) f_{\text{eq}, \ell}, \quad (38)$$

$$n \geq n^{(k-1)}, \quad (39)$$

$$\mathbf{m} \geq \mathbf{m}^{(k-1)}, \quad (40)$$

$$\text{mod}(n, 3) = 0, \quad (41)$$

$$\text{mod}(m_{\ell}, 3) = 0, \quad \ell = 1, \dots, L, \quad (42)$$

$$n \leq n^{(k-1)} + 30, \quad (43)$$

$$\delta^{\text{CV+S}}(r, \tilde{r}, \Theta_{n^{(k-1)}}, \Theta_{\mathbf{m}^{(k-1)}}, n, \mathbf{m}) \leq \delta_t, \quad (44)$$

where  $n_{\text{eq}}$  represents the number of equivalent simulations;  $f_{\text{eq}, \ell}$  is the ratio between the time of one evaluation of the response using the  $\ell$ th LF model and the time of one evaluation of the response using the HF model;  $\text{mod}(\cdot, \cdot)$  denotes the modulo operation;  $\delta^{\text{CV+S}}(r, \tilde{r}, \Theta_{n^{(k-1)}}, \Theta_{\mathbf{m}^{(k-1)}}, n, \mathbf{m})$  in Eq. (44) is the maximum between the coefficients of variation associated with the estimators of the first three moments, which is calculated considering sample set sizes  $(n, \mathbf{m})$ , but whose co-moments are evaluated using the sample sets  $\Theta_{n^{(k-1)}}$  and  $\Theta_{\mathbf{m}^{(k-1)}}$ . Details for evaluating the maximum coefficient of variation in Eq. (44) are discussed in [Appendix D](#). From the optimization problem described above, note that Eq. (37) simply corresponds to the numerical effort associated with the evaluation of the HF and LF models, which is expressed in terms of the number of equivalent simulations  $n_{\text{eq}}$ . This number  $n_{\text{eq}}$  expresses the total numerical cost of running the Control Variates approach in terms of the number of HF evaluations. In this sense, the ratios  $f_{\text{eq}, \ell}$  transform the efforts associated with the evaluation of each LF model to an equivalent number with respect to the HF model, as shown in Eq. (38). The constraints in Eqs. (39) and (40) ensure that the optimal values for the sample set sizes  $(n, \mathbf{m})$  are always equal or larger than the actual number of evaluations already carried out. This ensures that previous calculations are always included within the analysis. The role of the constraints in Eqs. (41) and (42) is ensuring that the sample set sizes  $(n, \mathbf{m})$  are always divisible by 3, such that the Splitting technique can be applied. The constraint in Eq. (43) limits the growth of  $n$  between iterations to at most 30 samples. This condition is introduced to avoid excessive increases in the number of HF evaluations due to inaccurate co-moment estimations, a phenomenon that may appear especially in early iterations, when few samples are available. The specific value of 30 has been adopted as a practical lower bound to ensure a minimally meaningful statistical representation within each update, while still keeping the number of HF evaluations computationally affordable. Finally, the constraint in Eq. (44) ensures that the coefficient of variation associated with the estimators of the first three moments remains below the target threshold  $\delta_t$ .

The optimization problem in Eqs. (37)–(44) corresponds to integer programming and can be solved using any appropriate algorithm. In this sense, please recall that while the optimization problem is solved, no evaluations of the HF or LF models take place. This is because co-moments are estimated with the initial sample sets  $\Theta_{n^{(k-1)}}$  and  $\Theta_{\mathbf{m}^{(k-1)}}$ . Hence, the solution of the optimization problem does not pose a major numerical effort, as both the objective function and constraints are explicit functions of  $n$  and  $\mathbf{m}$ . Numerical experience indicates that the optimization problem can be also solved considering that  $n$  and  $\mathbf{m}$  are continuous variables and then, ceiling the results to the closest multiple of 3 (to apply the Splitting technique). Alternatively, the problem could be formulated directly with discrete design variables; however, the continuous formulation adopted here has proven sufficiently accurate for the purposes of this study.

### 3.6. Implementation

The practical implementation of the approach involving Control Variates with Splitting requires a number of steps, which are summarized in the following.

1. Given a certain physical problem, establish a high-fidelity (HF) model that accurately characterizes its behavior. Describe uncertain input parameters through probability distributions and identify the response of interest  $r$  of the system.
2. Establish one or more low-fidelity (LF) models,  $\tilde{r}_{\ell}$ ,  $\ell = 1, \dots, L$ , that provide approximate but numerically inexpensive representations of the system's response.
3. Select the initial sample set sizes  $(n^{(0)}, \mathbf{m}^{(0)})$  such that  $n^{(0)}$  and each component of  $\mathbf{m}^{(0)}$  are multiples of 3. It is recommended to select these sizes to be relatively small. Select the target

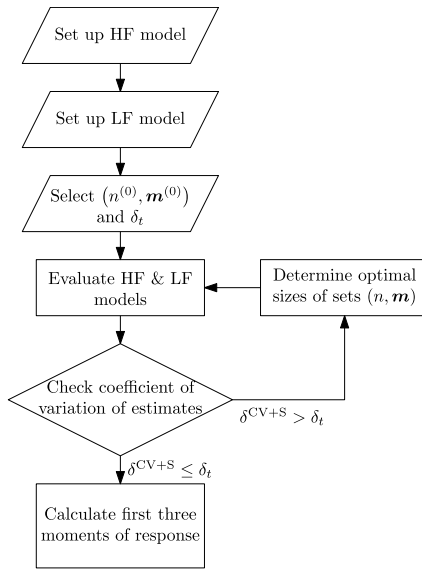


Fig. 1. Flowchart of approach using high- and low-fidelity models.

coefficient of variation  $\delta_i$  for estimating the first three statistical moments. Set  $k = 1$ .

4. Evaluate the response considering the high-fidelity (HF) model for the shared sample set  $\Theta_{n(k-1)}$  and the responses of all low-fidelity (LF) models  $\tilde{r}_\ell$ ,  $\ell = 1, \dots, L$ , for the shared sample sets  $\Theta_{n(k-1)}$  and their corresponding independent sample sets  $\Theta_{m_\ell(k-1)}$ .
5. Evaluate the constraint associated with the coefficient of variation in Eq. (44) assuming that  $n = n^{(k-1)}$  and  $m = m^{(k-1)}$ . If the constraint is fulfilled, go to step 7. Otherwise, go to step 6.
6. Solve the optimization problem in Eqs. (37)–(44) to determine the optimal sample set sizes  $(n^{(k)}, m^{(k)})$ . Set  $k = k + 1$  and return to step 4.
7. Considering the sample sets  $\Theta_{n(k-1)}$  and  $\Theta_{m(k-1)}$  and the corresponding evaluations of the response using the HF and LF models, evaluate the first three moments (see Eqs. (22), (27), and (32)) of the response, as well as the respective variances of these estimators (see Eqs. (25), (29), and (34)).

From the above algorithm, note that steps 4 to 6 are applied iteratively. The reason is that the optimization problem in Eqs. (37)–(44) predicts the optimal sizes for the sample sets  $(n, m)$  (see step 6), but then, the actual coefficient of variation associated must be verified (see step 5). The overall workflow of the proposed approach is summarized in Fig. 1.

## 4. Examples

### 4.1. General remarks

This Section illustrates the application of the scheme described previously for estimating first-, second-, and third-order moments of a certain system of interest. Three examples are chosen, where each of them serves a different purpose. The example in Section 4.2 involves a very simple analytic function. Such an example possesses a closed-form solution and it is ideal for conducting numerical tests regarding the bias correction capabilities of the Control Variates with Splitting strategy. The example in Section 4.3 illustrates the application of the proposed approach into a seepage analysis problem involving a medium-sized finite element model. This example offers an excellent testbed for illustrating numerical gains with the proposed approach. Finally, Section 4.4 presents a dynamic and nonlinear example based on the

Duffing oscillator. This problem involves a high-dimensional random input space and it is considerably more involved than the previous two examples. Indeed, this example involves two different low-fidelity models and hence, showcases the applicability of the framework discussed in this work.

### 4.2. Test example: Analytic function

#### 4.2.1. Description

This example involves the following analytic function:

$$r(\theta) = e^{3\theta}, \quad (45)$$

where  $r$  is the response of interest and  $\theta$  is an uncertain input parameter that follows a uniform distribution, i.e.,  $\theta \sim \mathcal{U}[0, 4]$ . The function in Eq. (45) is regarded as the high-fidelity model (HF) in this context.

Given the simplicity of the HF model, its first three moments can be calculated in closed form, yielding:

$$\mu'_1 = 1.356 \times 10^4, \quad \mu'_2 = 9.198 \times 10^8, \quad \mu'_3 = 7.984 \times 10^{13}.$$

To construct a LF model, the function in Eq. (45) is approximated by means of its second-order Taylor expansion about the point  $\theta_0 = 2$ , yielding:

$$\tilde{r}(\theta) = \frac{e^6}{2} (9\theta^2 - 30\theta + 26). \quad (46)$$

In this example, only one LF model is considered. The objective of this test example is solely to analyze the effect of the Splitting strategy on the bias of the estimators of the first three moments of the response, as discussed in detail in Section 4.2.2. Hence, optimal selection of the number of evaluations  $(n, m)$  of the high- and low-fidelity models is not further investigated and arbitrary numbers are selected for  $(n, m)$ . The optimal selection of the number of evaluations of the low- and high fidelity models is postponed for the subsequent two examples in Sections 4.3 and 4.4.

#### 4.2.2. Bias and the splitting strategy

The objective of this section is to evaluate the effect of the Splitting strategy on the bias of the estimators of the first three moments of the response  $r$ , defined in Eq. (45). Two approaches are considered:

- Applying the Control Variates (CV) method without Splitting. In this case, the estimators are computed using Eq. (16) for the mean, and the following expressions for the second and third central moments:

$$\hat{\mu}_2^{\text{CV}}(r, \tilde{r}; \Theta_n, \Theta_m) = \hat{\mu}_2(r; \Theta_n) - \gamma^* [\hat{\mu}_2(\tilde{r}; \Theta_n) - \hat{\mu}_2(\tilde{r}; \Theta_m)], \quad (47)$$

$$\hat{\mu}_3^{\text{CV}}(r, \tilde{r}; \Theta_n, \Theta_m) = \hat{\mu}_3(r; \Theta_n) - \eta^* [\hat{\mu}_3(\tilde{r}; \Theta_n) - \hat{\mu}_3(\tilde{r}; \Theta_m)], \quad (48)$$

where the control parameters  $\gamma^*$  and  $\eta^*$  are calculated using the sets of samples  $\Theta_n$  and  $\Theta_m$ . That means that no splitting is applied.

- Applying the Control Variates with Splitting (CV+S) method. In this case, the estimators for the first three moments are computed using Eqs. (22), (27), and (32).

To compare both strategies, the following setup is used. The sample sizes  $n$  and  $m$  are selected such that  $n \in \{72, 90, 117, 147, 186, 237, 300\}$  and  $m = 20n$ . For each pair  $(n, m)$ , the three moments of the response  $r$  are estimated using both CV and CV+S. In order to eliminate the effect of sampling variability, all estimators are averaged over  $10^6$  independent repetitions.

The results are reported in Fig. 2, together with the exact values of the moments, which are known in this example.

Fig. 2 shows that the estimators obtained using CV exhibit noticeable bias for small values of  $n$ , whereas those obtained using CV+S are unbiased across all sample sizes, with only small deviations due to

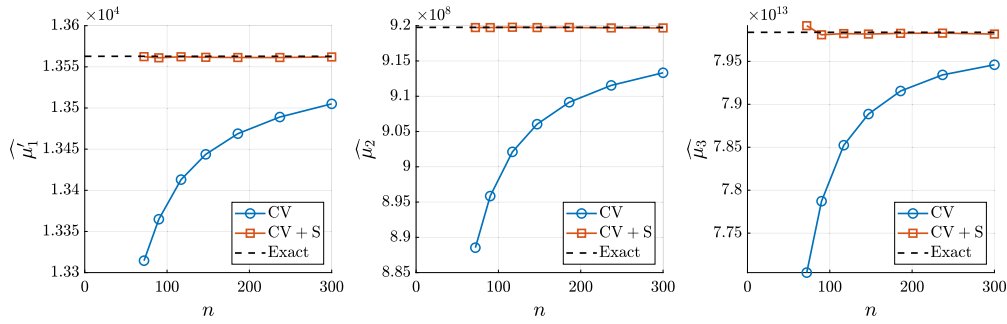


**Fig. 2.** Example 1 – Estimates of the first raw moment  $\hat{\mu}_1$  and the second and third central moments  $\hat{\mu}_2$  and  $\hat{\mu}_3$  as a function of the number of high-fidelity samples  $n$ .

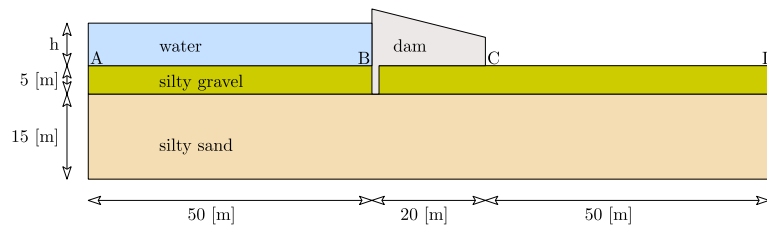


**Fig. 3.** Example 2 – Schematic representation of dam.

sampling variability. These results confirm that the Splitting strategy is effective in removing the bias present in the standard CV approach. In fact, they are in full agreement with the theoretical analysis presented in [Appendix C](#), which proves that the CV+S estimators are unbiased. This indicates that the proposed CV+S method provides highly accurate estimators even for small sample sizes, as it successfully eliminates the bias.

#### 4.3. Example: Confined seepage below an impermeable dam

##### 4.3.1. Description

This example involves estimating the first three moments of the seepage flow below an impermeable dam. This example is drawn from [\[62\]](#) and involves a medium-sized finite element model and few random variables. Such model is chosen on purpose to focus on assessing the performance of Control Variates with Splitting. A schematic representation of the problem is depicted in [Fig. 3](#).

The dam possesses a cutoff wall and it retains a water column of height  $h$ , which is an uncertain parameter modeled as a uniform distribution  $U[7, 10]$  [m]. The dam lies over two layers of permeable soil, whose horizontal and vertical permeabilities are modeled as lognormal random variables with mean and standard deviation as described in [Table 2](#). The coefficient of variation associated with each permeability is equal to 120%, reflecting the high uncertainty associated with this parameter in practical applications [\[63\]](#). Hence, the total number of uncertain input variables in this case is equal to 5 (water column height and the vertical and horizontal permeabilities of each of the two soil layers).

It is assumed that the seepage phenomenon can be described by the Laplace partial differential equation. A finite element model comprising 3413 nodes, 1628 quadratic triangular elements and  $n_d = 3128$  degrees-of-freedom is built to solve the partial differential equation and calculate the seepage flow [\[1\]](#). Such solution considering finite

**Table 2**

Example 2 – Mean value and standard deviation of permeability in different soil layers (CoV = 120%).

Soil layer	Permeability	Mean [m/s]	Std. deviation [m/s]
Silty sand	horizontal	$5.0 \times 10^{-7}$	$6.0 \times 10^{-7}$
	vertical	$2.0 \times 10^{-7}$	$2.4 \times 10^{-7}$
Silty gravel	horizontal	$5.0 \times 10^{-6}$	$6.0 \times 10^{-6}$
	vertical	$2.0 \times 10^{-6}$	$2.4 \times 10^{-6}$

elements corresponds to the HF model for this example. The boundary conditions involve no flow in all boundaries, except for boundary AB, where the boundary condition is the water height  $h$ , and boundary CD, where the water height is zero. The seepage flow  $q$  is quantified considering a unit width of the dam, so its units are  $[m^3/s/m]$ . To apply the framework of Control Variates with Splitting, a single low-fidelity (LF) model is constructed. This LF model is built by projecting the equations associated with the finite element formulation onto a reduced basis using a standard Galerkin procedure [\[1\]](#). The reduced basis is constructed using the nominal solution and its first-order derivatives with respect to the uncertain input parameters of the model, evaluated at a selected expansion point [\[64,65\]](#). Numerical experience [\[65\]](#) has shown that choosing this expansion point as the expected value of the input random variables produces good results. This leads to a reduced basis with  $n_R = 6$  terms, as the basis is constructed with the nominal solution of the problem (one term) and the first-order partial derivatives (five terms). All the previous terms are calculated for the so-called nominal solution of the seepage problem, involving the expected values of the different input random parameters. Note that  $n_R$  is much smaller than the dimension  $n_d = 3128$  associated with the high-fidelity (HF) model, where  $n_R$  corresponds to the dimension of the reduced subspace and  $n_d$  to the number of degrees of freedom of the FE model. This reduction implies solving a linear system of size  $n_R \times n_R$  instead of



**Table 3**

Example 2 – Selection of the optimal sizes for the sample sets  $(n, m)$  as a function of the target coefficient of variation  $\delta_i$ . Physical units of the moments are omitted for conciseness.

$n^{(0)}$	$m^{(0)}$	$\delta_i$	$n^{\text{opt}}$	$m^{\text{opt}}$	$n_{\text{eq}}$	$\hat{\mu}_1$	$\text{CoV}[\hat{\mu}_1]$	$\hat{\mu}_2$	$\text{CoV}[\hat{\mu}_2]$	$\hat{\mu}_3$	$\text{CoV}[\hat{\mu}_3]$
60	60	0.20	300	17 955	466.0	$2.0 \times 10^{-6}$	0.01	$1.6 \times 10^{-12}$	0.06	$4.6 \times 10^{-18}$	0.17
300	17 955	0.15	300	24 555	526.0	$2.0 \times 10^{-6}$	0.01	$1.6 \times 10^{-12}$	0.03	$4.5 \times 10^{-18}$	0.14
300	24 555	0.10	540	50 955	1 008.1	$2.0 \times 10^{-6}$	0.01	$1.6 \times 10^{-12}$	0.02	$3.8 \times 10^{-18}$	0.10
540	50 955	0.05	2 622	354 312	5 866.8	$2.0 \times 10^{-6}$	<0.01	$1.5 \times 10^{-12}$	0.02	$3.9 \times 10^{-18}$	0.05

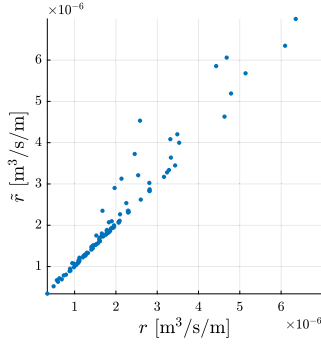


**Fig. 4.** Example 2 – Scatter plot of the seepage flow evaluated with the high-fidelity model (HF,  $r$ ) and the low-fidelity model (LF,  $\bar{r}$ ) using 100 samples.

$n_d \times n_d$ , which explains the much lower computational cost of the LF model. Thus, evaluating the LF model is about 110 times faster than the HF model. This ratio can be expressed as the equivalent cost factor  $f_{\text{eq}} = 1/110$ , which is used to compute the equivalent number of high-fidelity model evaluations. Furthermore, the LF model offers a good surrogate for the HF model, as noted from Fig. 4. This figure contains pairs of values of the seepage flow calculated considering the high-fidelity model (denoted as  $r$ ) and the low-fidelity model (denoted as  $\bar{r}$ ) for 100 samples of the random variables associated with the problem. It is observed that these pairs lie very close to a line with an inclination of  $45^\circ$ , indicating that the low-fidelity model is capable of producing accurate values of the seepage flow when compared to the high-fidelity model.

#### 4.3.2. Results

The approach based on Control Variates with Splitting is applied to estimate the first three order moments of the seepage flow. The sizes of the initial sample sets are selected as  $(n^{(0)}, m^{(0)}) = (60, 60)$  (see Sections 3.5 and 3.6). The reason for selecting the specific size of 60 is ensuring that when the Splitting strategy is applied, each subset of samples has at least 20 samples. This allows an appropriate estimation of the associated co-moments. Furthermore, the maximum allowable coefficient of variation is set as  $\delta_i = 20\%$  (see Eq. (44)). The results obtained are depicted in the second row of Table 3. Please note that physical units have been omitted for conciseness in that Table; nevertheless, recall that the units of the response of interest are  $[\text{m}^3/\text{s}/\text{m}]$ , which represent seepage flow per meter. The results from Table 3 allow to draw several important observations. First, it is observed that from the three moments being calculated, the third-order moment is the one possessing the largest coefficient of variation. Recall that the coefficient of variation of a moment (denoted as  $\text{CoV}[\cdot]$  in the Table) represents the standard deviation of the estimator divided by its expected value. The fact that the largest coefficient of variation is associated with the third-order moment of the response makes sense from a practical viewpoint, as usually high-order moments are more challenging to estimate than their low-order counterparts. Regarding the number of evaluation of the high- and low-fidelity models, it is observed that from the initial

sample size  $(n^{(0)}, m^{(0)}) = (60, 60)$ , the optimal number of evaluations to evaluate the sought moments is  $(n^{\text{opt}}, m^{\text{opt}}) = (300, 17\,955)$ . Thus, the number of evaluations of the LF model grows much more than that of the HF model. This was expected, as the LF model offers a good approximation with respect to the HF model while being faster to evaluate.

In a next step, the estimation of the first three order moments of the seepage flow is investigated by considering successively smaller target coefficient of variations  $\delta_i$ . Specifically, the values of 15%, 10% and 5% are considered. The initial number of evaluations of the low- and high-fidelity models for each case is taken as the optimal one associated with the previous target value of the coefficient of variation investigated. That is, when determining the sought moments with a target coefficient of variation of 15%, the initial number of evaluations is taken as the optimal number found when evaluating the moments for a target coefficient of variation of 20%. The results obtained are shown in Table 3 in the third, fourth and fifth rows. It is observed that the smaller the target coefficient of variation, the larger the number of equivalent simulations  $n_{\text{eq}}$  becomes. This is an expected result, as higher levels of precision usually go hand-in-hand with larger numerical efforts. Furthermore, the coefficient of variation associated with the third-order moment always remains the highest among the three analyzed moments.

As a last step and to validate the results of Table 3, the estimates of the moments produced with the more stringent target value of the coefficient of variation (that is,  $\delta_i = 5\%$ ) are compared against those produced using Monte Carlo simulation with the HF model only. These results are shown in Table 4, where it is noted that 50 000 simulations of the HF model are required to match the target coefficient of variation of 5%. When comparing the results in Tables 3 and 4, it is observed that there is an excellent match of the first three moments of the seepage flow calculated with Control Variates with Splitting (CV+S) and Monte Carlo simulation (MCS). While MCS requires  $n_{\text{MCS}} = 50\,000$  high-fidelity simulations to meet the precision target  $\delta_i = 0.05$ , CV+S achieves the same precision with only  $n = 2\,622$  and  $m = 354\,312$ , corresponding to  $n_{\text{eq}} = 5\,866.8$  equivalent simulations. This implies that CV+S is approximately 8.5 times faster than MCS for the same level of precision.

As a final comment, it is important to note that from the point of view of the results obtained, the seepage flow is a strongly non-Gaussian random variable. From the obtained moments, the skewness (which is equal to the third moment over the cube of the standard deviation) is above 2. This reveals that the right tail of the seepage flow is (significantly) heavier than the left.

#### 4.4. Application example: Nonlinear dynamic system (Duffing oscillator)

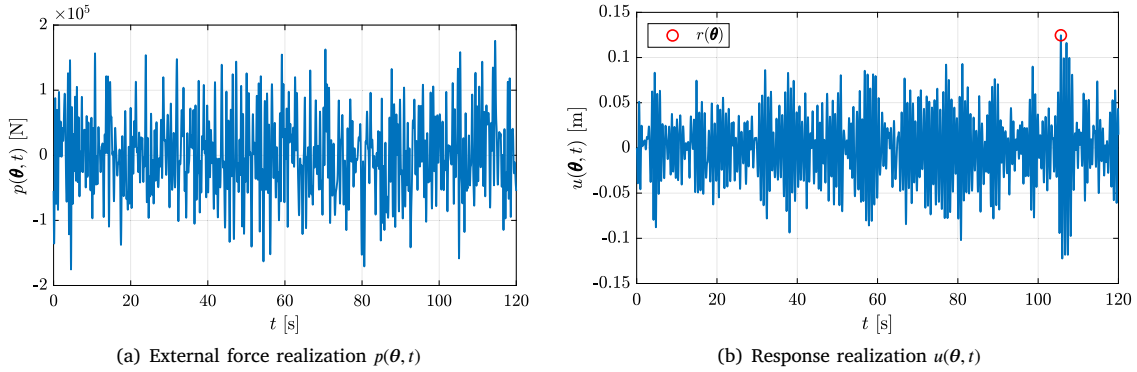
##### 4.4.1. Description

This example involves a nonlinear Duffing oscillator with one degree of freedom, subject to stochastic excitation. This is a classical benchmark for performing uncertainty quantification [66–69]. Its governing equation is:

$$m\ddot{u}(\theta, t) + c\dot{u}(\theta, t) + ku(\theta, t) + k_3u^3(\theta, t) = p(\theta, t), \quad (49)$$

**Table 4**Example 2 – Reference values from Monte Carlo simulation for a target coefficient of variation  $\delta_i = 0.05$ . Physical units of the moments are omitted for conciseness.

$\delta_i$	$n_{\text{MCS}}$	$m_{\text{MCS}}$	$n_{\text{eq}}$	$\hat{\mu}_1$	$\text{CoV}[\hat{\mu}_1]$	$\hat{\mu}_2$	$\text{CoV}[\hat{\mu}_2]$	$\hat{\mu}_3$	$\text{CoV}[\hat{\mu}_3]$
0.05	50 000	0	50 000.0	$2.0 \times 10^{-6}$	<0.01	$1.5 \times 10^{-12}$	0.01	$3.8 \times 10^{-18}$	0.05

**Fig. 5.** Example 3 – One realization of the stochastic force  $p(\theta, t)$  and the corresponding system response  $u(\theta, t)$  in the Duffing oscillator.

where  $u(\theta, t)$  is the displacement at time  $t$ ,  $m = 6 \times 10^4$  kg is the mass,  $c = 2\zeta\sqrt{km}$  is the damping coefficient with damping ratio  $\zeta = 0.05$ ,  $k = 5 \times 10^6$  N/m is the linear stiffness, and  $k_3 = 0.4k = 2 \times 10^6$  N/m<sup>3</sup> is the cubic stiffness. The initial conditions are zero displacement and velocity:  $u(\theta, 0) = \dot{u}(\theta, 0) = 0$ . The external excitation  $p(\theta, t)$  is a stochastic force modeled as a finite sum of sinusoidal components with random phase:

$$p(\theta, t) = -m \sum_{i=1}^n \sqrt{4S\Delta\omega} \cos(\omega_i t + \theta_i), \quad (50)$$

where  $n = 300$  is the number of input random variables,  $S = 0.03$  m<sup>2</sup>/s<sup>3</sup> is the white noise intensity, and  $\Delta\omega = \omega_{\max}/n$  with  $\omega_{\max} = 15$  rad/s. The random variables  $\theta_i \sim U[0, 2\pi]$  represent uniformly distributed random phase angles, and the frequencies are defined as  $\omega_i = \Delta\omega \cdot i$ . This configuration results in a high-dimensional input space, with 300 independent random variables. The simulation time is  $T = 120$  s. Two low-fidelity (LF) models are considered in addition to the high-fidelity (HF) model:

- The *high-fidelity model* (HF), with time step  $\Delta t_{\text{HF}} = 0.01412$  s and  $n_t^{\text{HF}} = 8501$  time steps.
- The *low-fidelity model* LF<sub>1</sub>, with time step  $\Delta t_{\text{LF}_1} = 0.10$  s and  $n_t^{\text{LF}_1} = 1201$  time steps.
- The *low-fidelity model* LF<sub>2</sub>, with time step  $\Delta t_{\text{LF}_2} = 0.16$  s and  $n_t^{\text{LF}_2} = 751$  time steps.

The quantity of interest is the maximum absolute displacement over the simulation horizon, defined as:

$$r(\theta) = \max_{t \in [0, T]} |u(\theta, t)|, \quad (51)$$

where  $|\cdot|$  denotes absolute value. This response is evaluated using the HF model and the two LF models, yielding the outputs  $r$ ,  $\tilde{r}_1$ , and  $\tilde{r}_2$ , respectively. To provide a quantitative idea of how the stochastic input loading and dynamic time response look like, Fig. 5(a) shows a selected realization of the loading while its corresponding response is shown in Fig. 5(b). The response of interest  $r$  is marked with a circle in the plot on the right and it corresponds to the maximum value of the displacement (in absolute value).

To apply Control Variates with Splitting (CV+S), it is important to assess how close the HF response  $r$  and the LF responses  $\tilde{r}_\ell$ ,  $\ell = 1, 2$ , are. Fig. 6 presents scatter plots comparing  $r$  with each LF response for 100 random input realizations.

Figs. 6(a) and (b) show that both LF models have a reasonable agreement with the HF model, but this agreement is stronger for LF<sub>1</sub>. However, the relative cost of LF<sub>1</sub> corresponds to a speed-up of 44.4 with respect to the HF model, i.e.  $f_{\text{eq},1} = 1/44.4$ , while LF<sub>2</sub> has a larger speed-up of 102.4, i.e.  $f_{\text{eq},2} = 1/102.4$ . Therefore, LF<sub>1</sub> provides higher accuracy, whereas LF<sub>2</sub> offers superior computational efficiency.

#### 4.4.2. Results

The estimates for the first three moments of the maximum displacement of the Duffing oscillator are presented in this section. As in the previous example, the initial sample sizes are set to  $(n^{(0)}, m^{(0)}) = (60, [60 \ 60]^T)$ , and the target coefficient of variation is set as  $\delta_i = 20\%$ . The estimates obtained for the first three moments along with the corresponding coefficients of variation are reported in the second row of Table 5. As in the previous example, physical units of the moments are omitted, but it should be reminded that the maximum displacement is measured in [m]. The results obtained show that the third order moment possesses the highest coefficient of variation. Moreover, the optimal number of evaluations of the HF model increases modestly in comparison with its initial value (that is, from  $n^{(0)} = 60$  to  $n^{\text{opt}} = 75$ ), while the LF models are evaluated a large number of times ( $m_1^{\text{opt}} = 498$ ,  $m_2^{\text{opt}} = 3423$ ). Hence, Control Variates with Splitting leverages significantly the LF models.

Following the strategy considered in the previous example, the target coefficient of variation used for estimating the first three order moments is reduced from 20% to 5% in intervals of 5%. Again, the optimal sample sizes associated with one target coefficient of variation are used as the initial sample size for estimating the sought moments for the next smallest target coefficient of variation. The results obtained are shown in the third, fourth and fifth rows of Table 5. It is observed again that the smaller the target coefficient of variation, the larger the number of equivalent simulations required. For all cases studied, Control Variates with Splitting is capable of leveraging the LF models.

In addition, the results obtained with Control Variates with Splitting (CV+S) are compared against those obtained with Monte Carlo

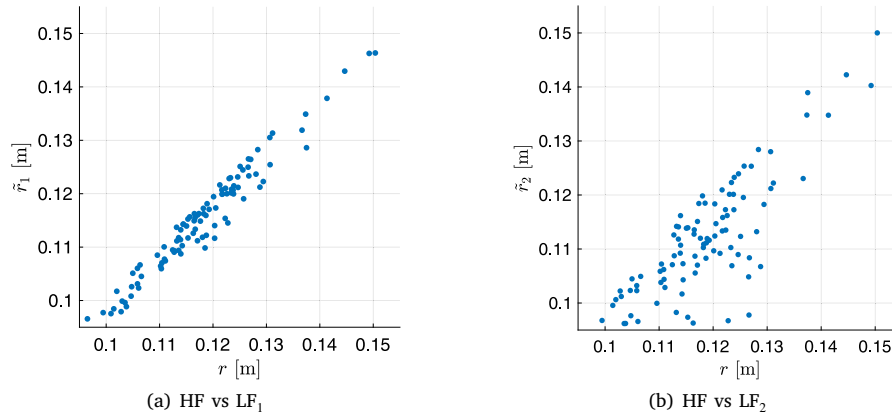


**Fig. 6.** Example 3 – Scatter plots of the maximum displacement evaluated with the high-fidelity model (HF,  $r$ ) and the low-fidelity models (LF<sub>1</sub>, LF<sub>2</sub>) using 100 samples.

**Table 5**

Example 3 – Selection of the optimal sizes for the sample sets ( $n, m$ ) as a function of the target coefficient of variation  $\delta_t$ . Physical units of the moments are omitted for conciseness.

$n^{(0)}$	$m_1^{(0)}$	$m_2^{(0)}$	$\delta_t$	$n^{\text{opt}}$	$m_1^{\text{opt}}$	$m_2^{\text{opt}}$	$n_{\text{eq}}$	$\hat{\mu}_1^t$	$\text{CoV}[\hat{\mu}_1^t]$	$\hat{\mu}_2$	$\text{CoV}[\hat{\mu}_2]$	$\hat{\mu}_3$	$\text{CoV}[\hat{\mu}_3]$
60	60	60	0.20	75	498	3423	122.1	$1.2 \times 10^{-1}$	$<0.01$	$1.4 \times 10^{-4}$	0.06	$1.4 \times 10^{-6}$	0.20
75	498	3423	0.15	105	2148	3834	194.2	$1.2 \times 10^{-1}$	$<0.01$	$1.4 \times 10^{-4}$	0.04	$1.4 \times 10^{-6}$	0.15
105	2148	3834	0.10	129	8166	3834	354.5	$1.2 \times 10^{-1}$	$<0.01$	$1.3 \times 10^{-4}$	0.03	$1.3 \times 10^{-6}$	0.09
129	8166	3834	0.05	1359	40008	13530	2436.1	$1.2 \times 10^{-1}$	$<0.01$	$1.4 \times 10^{-4}$	0.02	$1.3 \times 10^{-6}$	0.05

**Table 6**

Example 3 – Reference values from Monte Carlo simulation for a target coefficient of variation  $\delta_t = 0.05$ . Physical units of the moments are omitted for conciseness.

$\delta_t$	$n_{\text{MCS}}$	$m_{\text{MCS}}$	$n_{\text{eq}}$	$\hat{\mu}_1^t$	$\text{CoV}[\hat{\mu}_1^t]$	$\hat{\mu}_2$	$\text{CoV}[\hat{\mu}_2]$	$\hat{\mu}_3$	$\text{CoV}[\hat{\mu}_3]$
0.05	15000	0	15000.0	$1.2 \times 10^{-1}$	$<0.01$	$1.4 \times 10^{-4}$	0.01	$1.3 \times 10^{-6}$	0.05

simulation (MCS) for estimating the sought moments of the response for a target coefficient of variation of 5%. The results obtained for MCS are shown in Table 6. Comparing both approaches highlights the efficiency gains enabled by CV+S. To achieve the same precision target  $\delta_t = 0.05$ , MCS requires 15000 high-fidelity simulations, whereas CV+S attains the same level of precision using only 1359 high-fidelity samples, together with  $m_1^{\text{opt}} = 40008$  and  $m_2^{\text{opt}} = 13530$  low-fidelity samples, yielding a total equivalent cost of  $n_{\text{eq}} = 2436.1$ . This translates into a speed-up factor of roughly 6.2, demonstrating the advantage of CV+S.

To investigate the influence of the number of low-fidelity models, an additional study was conducted considering only the model LF<sub>1</sub>. The corresponding results are reported in Table 7 and compared with those obtained when both LF<sub>1</sub> and LF<sub>2</sub> are used (Table 5). They show that adding a second LF model systematically reduces the equivalent cost required to reach a given target precision. The efficiency gain ranges from about 6% to 38%, but it does not increase monotonically with the target CoV. A closer inspection of the optimal sample sizes in Table 5 reveals that the role of each LF model evolves with the target precision: for larger tolerances ( $\delta_t = 0.20$ ), the estimator heavily exploits the cheaper but less correlated model LF<sub>2</sub>, while for smaller tolerances, the contribution of LF<sub>2</sub> decreases and the more correlated model LF<sub>1</sub> becomes dominant. This behavior suggests that the marginal benefit of including multiple LF models depends on both their correlation with the HF model and their relative computational costs, and that the

balance between these two aspects is automatically captured by the optimization of the sample sizes within the CV+S framework.

Finally, by analyzing the results obtained in this example, it is noted that the maximum displacement is moderately non-Gaussian, as its skewness is approximately 0.8. As in the previous example, this can play a significant role for practical design. For example, a Gaussian approximation could lead to, e.g. non-conservative reliability estimates.

As an additional remark, it should be noted that the Duffing oscillator possesses a single-degree-of-freedom. Nevertheless, the proposed estimator can cope with models involving a large number of degrees-of-freedom. For example, the high-fidelity model may correspond to a fine discretization (with many degrees of freedom), while one or more low-fidelity models could be coarser meshes. The numerical cost of the estimator depends mainly on the cost of solving the high-fidelity model and the correlation with the low-fidelity models. The total cost scales linearly with the sample sizes (see Eq. (38)). Although splitting introduces a further partition of the sample sets to remove bias, this only adds a constant overhead, so the linear scaling is preserved. If the low-fidelity models are much cheaper and very correlated with the high-fidelity one, the use of control variates with splitting is very useful in large-scale problems. Finally, the extension of the proposed estimator to these more complex structural models with multiple degrees of freedom remains an open topic for future investigation.

**Table 7**

Example 3 – Selection of the optimal sizes for the sample sets  $(n, m_1)$  as a function of the target coefficient of variation  $\delta_i$  when only the low-fidelity model  $LF_1$  is used. Physical units of the moments are omitted for conciseness.

$n^{(0)}$	$m_1^{(0)}$	$\delta_i$	$n^{\text{opt}}$	$m_1^{\text{opt}}$	$n_{\text{eq}}$	$\hat{\mu}_1$	$\text{CoV}[\hat{\mu}_1]$	$\hat{\mu}_2$	$\text{CoV}[\hat{\mu}_2]$	$\hat{\mu}_3$	$\text{CoV}[\hat{\mu}_3]$
60	60	0.20	72	2778	136.2	$1.2 \times 10^{-1}$	<0.01	$1.4 \times 10^{-4}$	0.04	$1.3 \times 10^{-6}$	0.20
72	2778	0.15	102	5082	218.8	$1.2 \times 10^{-1}$	<0.01	$1.4 \times 10^{-4}$	0.04	$1.3 \times 10^{-6}$	0.15
102	5082	0.10	309	11 514	575.3	$1.2 \times 10^{-1}$	<0.01	$1.4 \times 10^{-4}$	0.03	$1.1 \times 10^{-6}$	0.10
309	11 514	0.05	1545	44 799	2588.8	$1.2 \times 10^{-1}$	<0.01	$1.4 \times 10^{-4}$	0.02	$1.3 \times 10^{-6}$	0.05

## 5. Conclusions

This paper has explored the application of Control Variates with Splitting for estimating the first three statistical moments (mean, variance, and third central moment) of the response of systems whose outputs are uncertain. The scheme combines high- and low-fidelity simulations. By leveraging the ability of the low-fidelity models to approximate the high-fidelity one, the approach reduces the numerical cost required to reach a prescribed level of estimation precision. The latter assertion holds when compared to standard Monte Carlo simulation that relies solely on the high-fidelity model.

There are two main contributions of this work. First, explicit expressions are provided for the estimators of the first three moments of the response as well as for the variances of these estimators. Calculating these three moments together is extremely relevant, as they may reveal the degree of non-Gaussianity of the response of a system. This plays a major role for decision-making, as using a Gaussian approximation based on second-order moments alone may lead to non-conservative reliability estimates. Second, the application of the Splitting technique ensures that the resulting estimators are unbiased, even when the same samples are used to compute both the estimators and the control parameters. This is a significant advantage, as the Splitting approach does not entail additional evaluations of the low- or high-fidelity models.

The approach combining Control Variates with Splitting has been successfully demonstrated in linear static and nonlinear dynamic systems. The latter example is particularly relevant, as it involves a high-dimensional random input space that would be challenging to address with, e.g. traditional surrogate models. In addition, it is important to note that the expressions derived for Control Variates with Splitting in this work are applicable irrespective of the type of underlying physical model. Hence, the approach discussed in this work is applicable to a wide range of problems. In this sense, the most important requirement is that one or more low-fidelity models approximate the high-fidelity one sufficiently well. This holds independent of how the low-fidelity models are constructed.

The approach investigated in this work focuses on scalar responses only, with a potential future research path consisting of extending its applicability toward vector-valued responses. In addition, extending the proposed estimator to more complex structural models with multiple degrees of freedom remains an open topic for future investigation.

## CRedit authorship contribution statement

**Cristóbal H. Acevedo:** Writing – review & editing, Software, Methodology, Funding acquisition, Formal analysis, Conceptualization. **Marcos A. Valdebenito:** Writing – review & editing, Writing – original draft, Supervision, Methodology, Formal analysis, Conceptualization. **Iván V. González:** Writing – review & editing, Methodology, Funding acquisition, Formal analysis, Conceptualization. **Héctor A. Jensen:** Writing – review & editing, Methodology, Funding acquisition, Formal analysis, Conceptualization. **Matthias G.R. Faes:** Writing – review & editing, Methodology, Funding acquisition, Formal analysis, Conceptualization.

## Declaration of competing interest

The author Matthias Faes is an Associate Editor of this journal. In accordance with policy, Matthias Faes was blinded to the entire peer review process.

## Acknowledgments

This research is partially funded by ANID (National Agency for Research and Development, Chile) under grant number 1240013 and its graduate scholarship program *CONICYT-PFCHA/MagisterNacional/2019-22191834* and *CONICYT-PFCHA/MagisterNacional/2017-22171799* as well as by the Deutsche Forschungsgemeinschaft (DFG, German Research Foundation) under project number 527637016, and by the State Key Laboratory of Disaster Reduction in Civil Engineering, Tongji University, under project number SLDRCE24-02. This support is gratefully acknowledged by the authors.



## Appendix A. Estimation of central co-moments

The expressions for estimating the mean, variance, and third central moment (and the variance of these estimators) with Control Variates depend on central moments and co-moments. For a single model response  $y$ , the central moment of order  $p$  is defined as:

$$\mu_p(y) := \mathbb{E}[(y - \mathbb{E}[y])^p], \quad (\text{A.1})$$

where  $\mathbb{E}[\cdot]$  denotes expected value of the argument. For two model responses  $y_a$  and  $y_b$ , the bivariate central co-moment of order  $(p, q)$  is defined as:

$$\mu_{p,q}(y_a, y_b) := \mathbb{E}[(y_a - \mathbb{E}[y_a])^p (y_b - \mathbb{E}[y_b])^q]. \quad (\text{A.2})$$

These quantities are estimated using Monte Carlo simulation by means of a sample set  $\Theta_g = \{\theta_{g,i}\}_{i=1}^g$  that contains  $g$  samples of the random variable vector  $\Theta$ . The specific expressions for the different co-moment estimators employed in this work have been deduced using the software *mathStatistica* [70] and are listed below. These expression have been validated numerically to confirm their unbiasedness. To define these expressions, we introduce the associated power sums, defined for one model response as

$$s_p(y; \Theta_g) := \sum_{i=1}^g (y(\theta_{g,i}))^p, \quad (\text{A.3})$$

and for two model responses as

$$s_{p,q}(y_a, y_b; \Theta_g) := \sum_{i=1}^g (y_a(\theta_{g,i}))^p (y_b(\theta_{g,i}))^q. \quad (\text{A.4})$$

For compactness, in the following we omit the explicit dependence of the power sums  $s_p$  and  $s_{p,q}$  on the models and sample sets. It is understood that each  $s_p$  and  $s_{p,q}$  is computed using the models and the group of samples associated with the corresponding central moment or co-moment under evaluation.

**Notation.** We define the estimation of any central co-moment of order  $(p, q)$  as a function  $F_{p,q}$  of the auxiliary quantities  $s_{i,j}$ :

$$\widehat{\mu}_{p,q} = F_{p,q}(s_{i,j}).$$

To express the reflected form compactly, we use the superscript (sym):

$$\widehat{\mu}_{p,q}^{(\text{sym})} := F_{p,q}(s_{i,j}^{(\text{sym})}), \quad s_{i,j}^{(\text{sym})} := s_{j,i}.$$

$$\widehat{\mu}_{1,1} = \frac{g s_{1,1} - s_{0,1} s_{1,0}}{(g-1)g} \quad (\text{A.5})$$

$$\begin{aligned} \widehat{\mu}_{2,2} = & \frac{1}{(g-3)(g-2)(g-1)g} \left( (-2g^2 + 4g - 6) s_{2,1} s_{0,1} + (-2g^2 + 4g - 6) s_{1,0} s_{1,2} + \right. \\ & (g^3 - 2g^2 + 3g) s_{2,2} + g s_{2,0} s_{0,1}^2 + 4g s_{1,0} s_{1,1} s_{0,1} + g s_{0,2} s_{1,0}^2 + \\ & \left. (6 - 4g) s_{1,1}^2 + (3 - 2g) s_{0,2} s_{2,0} - 3 s_{1,0}^2 s_{0,1} \right) \end{aligned} \quad (\text{A.6})$$

$$\begin{aligned} \widehat{\mu}_4 = & \frac{1}{(g-3)(g-2)(g-1)g} \left( (-4g^2 + 8g - 12) s_3 s_1 + (g^3 - 2g^2 + 3g) s_4 + \right. \\ & \left. 6g s_2 s_1^2 + (9 - 6g) s_2^2 - 3 s_1^4 \right) \end{aligned} \quad (\text{A.7})$$

The squared co-moments  $\mu_{1,1}^2$ ,  $\mu_2^2$ , and the co-moment product  $\mu_{2,0}\mu_{0,2}$  are estimated with the following expressions [70].

$$\begin{aligned} \widehat{\mu}_{1,1}^2 = & \frac{1}{(g-3)(g-2)(g-1)g} \left( (g^2 - 3g + 2) s_{1,1}^2 + (g - g^2) s_{2,2} + \right. \\ & (2 - 2g) s_{1,0} s_{1,1} s_{0,1} + (2g - 2) s_{2,1} s_{0,1} + (2g - 2) s_{1,0} s_{1,2} + \\ & \left. s_{1,0}^2 s_{0,1}^2 - s_{2,0} s_{0,1}^2 - s_{0,2} s_{1,0}^2 + s_{0,2} s_{2,0} \right) \end{aligned} \quad (\text{A.8})$$

$$\widehat{\mu}_2^2 = \frac{(g^2 - 3g + 3) s_2^2 + (g - g^2) s_4 - 2g s_2 s_1^2 + (4g - 4) s_3 s_1 + s_1^4}{(g-3)(g-2)(g-1)g} \quad (\text{A.9})$$

$$\begin{aligned} \widehat{\mu}_{2,0}\mu_{0,2} = & \frac{1}{(g-3)(g-2)(g-1)g} \left( (g^2 - 3g + 1) s_{0,2} s_{2,0} + (g - g^2) s_{2,2} + \right. \\ & (2 - g) s_{2,0} s_{0,1}^2 + (2g - 2) s_{2,1} s_{0,1} + (2 - g) s_{0,2} s_{1,0}^2 + \\ & \left. (2g - 2) s_{1,0} s_{1,2} + s_{1,0}^2 s_{0,1}^2 - 4 s_{1,0} s_{1,1} s_{0,1} + 2 s_{1,1}^2 \right) \end{aligned} \quad (\text{A.10})$$

The following provides the expressions for the central co-moments required for the estimation of the third-order moment and its coefficient of variation.

$$\widehat{\mu}_3 = \frac{2 s_1^3 - 3g s_1 s_2 + g^2 s_3}{(g-2)(g-1)g} \quad (\text{A.11})$$

$$\begin{aligned} \widehat{\mu}_6 = & \frac{1}{(g-5)(g-4)(g-3)(g-2)(g-1)g} \left[ -5 s_1^6 + 15g s_1^4 s_2 - 45(2g-5) s_1^2 s_2^2 \right. \\ & + 15(3g-10) s_2^3 - 20(g^2-6g+15) s_1^3 s_3 + 60(g^2-4g+5) s_1 s_2 s_3 \\ & \left. - 40(g^2-6g+10) s_3^2 + 15(g^3-8g^2+23g-10) s_1^2 s_4 \right] \end{aligned}$$

$$-15(g^3-8g^2+29g-40)s_2s_4-6(g^4-9g^3+31g^2-39g+40)s_1s_5 \\ +g(g^4-9g^3+31g^2-39g+40)s_6] \quad (\text{A.12})$$

$$\widehat{\mu_{3,3}} = \frac{1}{(g-5)(g-4)(g-3)(g-2)(g-1)g} [-5s_{0,1}^3s_{1,0}^3+3gs_{0,1}s_{0,2}s_{1,0}^3-(g^2-6g+15)s_{0,3}s_{1,0}^3 \\ +9gs_{0,1}^2s_{1,0}^2s_{1,1}-9(2g-5)s_{0,2}s_{1,0}^2s_{1,1}-18(2g-5)s_{0,1}s_{1,0}s_{1,1}^2+6(3g-10)s_{1,1}^3 \\ -9(g^2-6g+15)s_{0,1}s_{1,0}^2s_{1,2}+18(g^2-4g+5)s_{1,0}s_{1,1}s_{1,2}+3(g^3-8g^2+23g-10)s_{1,0}^2s_{1,3} \\ +3gs_{0,1}^3s_{1,0}s_{2,0}-9(2g-5)s_{0,1}s_{0,2}s_{1,0}s_{2,0}+3(g^2-4g+5)s_{0,3}s_{1,0}s_{2,0} \\ -9(2g-5)s_{0,1}^2s_{1,1}s_{2,0}+9(3g-10)s_{0,2}s_{1,1}s_{2,0}+9(g^2-4g+5)s_{0,1}s_{1,2}s_{2,0} \\ -3(g^3-8g^2+29g-40)s_{1,3}s_{2,0}-9(g^2-6g+15)s_{0,1}^2s_{1,0}s_{2,1}+9(g^2-4g+5)s_{0,2}s_{1,0}s_{2,1} \\ +18(g^2-4g+5)s_{0,1}s_{1,1}s_{2,1}-36(g^2-6g+10)s_{1,2}s_{2,1}+9(g^3-8g^2+23g-10)s_{0,1}s_{1,0}s_{2,2} \\ -9(g^3-8g^2+29g-40)s_{1,1}s_{2,2}-3(g^4-9g^3+31g^2-39g+40)s_{1,0}s_{2,3} \\ -(g^2-6g+15)s_{0,1}^3s_{3,0}+3(g^2-4g+5)s_{0,1}s_{0,2}s_{3,0}-4(g^2-6g+10)s_{0,3}s_{3,0} \\ +3(g^3-8g^2+23g-10)s_{0,1}^2s_{3,1}-3(g^3-8g^2+29g-40)s_{0,2}s_{3,1} \\ -3(g^4-9g^3+31g^2-39g+40)s_{0,1}s_{3,2}+g(g^4-9g^3+31g^2-39g+40)s_{3,3}] \quad (\text{A.13})$$

$$\widehat{\mu_3^2} = \frac{1}{(g-5)(g-4)(g-3)(g-2)(g-1)g} [4s_1^6-12gs_1^4s_2+9g(g-1)s_1^2s_2^2 \\ +(45g-60-9g^2)s_2^3+(12g+4g^2)s_1^3s_3+(120-90g+24g^2-6g^3)s_1s_2s_3 \\ +(25g^2-8g^3+g^4-10g-40)s_3^3+(-60+45g-21g^2)s_1^2s_4 \\ +(60-15g-15g^2+6g^3)s_2s_4+(-24+30g-12g^2+6g^3)s_1s_5 \\ +(4g-5g^2+2g^3-g^4)s_6] \quad (\text{A.14})$$

$$\widehat{\mu_2^3} = \frac{1}{(g-5)(g-4)(g-3)(g-2)(g-1)g} [-s_1^6+3gs_1^4s_2+(9g-15-3g^2)s_1^2s_2^2 \\ +(29g-30-9g^2+g^3)s_2^3+(20-12g)s_1^3s_3+(60-48g+12g^2)s_1s_2s_3 \\ +(30g-40-6g^2)s_3^3+(9g+3g^2-30)s_1^2s_4+(60-60g+21g^2-3g^3)s_2s_4 \\ +(36g-24-12g^2)s_1s_5+(4g-6g^2+2g^3)s_6] \quad (\text{A.15})$$

$$\widehat{\mu_{1,1}^3} = \frac{1}{(g-5)(g-4)(g-3)(g-2)(g-1)g} [-s_{0,1}^3s_{1,0}^3+3s_{0,1}s_{0,2}s_{1,0}^3-2s_{0,3}s_{1,0}^3 \\ +(3g-6)s_{0,1}^2s_{1,0}^2s_{1,1}+(6-3g)s_{0,2}s_{1,0}^2s_{1,1} \\ +(15g-18-3g^2)s_{0,1}s_{1,0}s_{1,1}^2+(26g-24-9g^2+g^3)s_{1,1}^3 \\ +(12-6g)s_{0,1}s_{1,0}^2s_{1,2}+(36-30g+6g^2)s_{1,0}s_{1,1}s_{1,2} \\ +(-12+6g)s_{1,0}^2s_{1,3}+3s_{0,1}^3s_{1,0}s_{2,0}-9s_{0,1}s_{0,2}s_{1,0}s_{2,0}+6s_{0,3}s_{1,0}s_{2,0} \\ +(6-3g)s_{0,1}^2s_{1,1}s_{2,0}+(-6+3g)s_{0,2}s_{1,1}s_{2,0}+(-12+6g)s_{0,1}s_{1,2}s_{2,0}+(12-6g)s_{1,3}s_{2,0} \\ +(12-6g)s_{0,1}^2s_{1,0}s_{2,1}+(-12+6g)s_{0,2}s_{1,0}s_{2,1}+(36-30g+6g^2)s_{0,1}s_{1,1}s_{2,1} \\ +(-36+30g-6g^2)s_{1,2}s_{2,1}+(-6-3g+3g^2)s_{0,1}s_{1,0}s_{2,2}+(36-48g+21g^2-3g^3)s_{1,1}s_{2,2} \\ +(-12+18g-6g^2)s_{1,0}s_{2,3}-2s_{0,1}^3s_{3,0}+6s_{0,1}s_{0,2}s_{3,0}-4s_{0,3}s_{3,0} \\ +(-12+6g)s_{0,1}^2s_{3,1}+(12-6g)s_{0,2}s_{3,1}+(-12+18g-6g^2)s_{0,1}s_{3,2} \\ +(4g-6g^2+2g^3)s_{3,3}] \quad (\text{A.16})$$

$$\widehat{\mu_2\mu_4} = \frac{1}{(g-5)(g-4)(g-3)(g-2)(g-1)g} [3s_1^6-9gs_1^4s_2+6g^2s_1^2s_2^2-15s_1^2s_2^2 \\ +(27g-30-6g^2)s_2^3+(20+4g^2)s_1^3s_3+(60-44g+12g^2-4g^3)s_1s_2s_3 \\ +(80g-80-28g^2+4g^3)s_3^3+(7g-30-6g^2-g^3)s_1^2s_4 \\ +(120-135g+53g^2-9g^3+g^4)s_2s_4+(66g-48-24g^2+6g^3)s_1s_5 \\ +(8g-11g^2+4g^3-g^4)s_6] \quad (\text{A.17})$$

$$\widehat{\mu_{0,2}\mu_{1,1}\mu_{2,0}} = \frac{1}{(g-5)(g-4)(g-3)(g-2)(g-1)g} [-s_{0,1}^3s_{1,0}^3+(g-2)s_{0,1}s_{0,2}s_{1,0}^3 \\ +(3-g)s_{0,3}s_{1,0}^3+(4+g)s_{0,1}^2s_{1,0}^2s_{1,1}+(-9+5g-g^2)s_{0,2}s_{1,0}^2s_{1,1} \\ +(2-4g)s_{0,1}s_{1,0}s_{1,1}^2+(-4+2g)s_{1,1}^3+(7-5g)s_{0,1}s_{1,0}^2s_{1,2} \\ +(6-4g+2g^2)s_{1,0}s_{1,1}s_{1,2}+(-2-g+g^2)s_{1,0}^2s_{1,3}+(g-2)s_{0,1}^3s_{1,0}s_{2,0} \\ +(1+3g-g^2)s_{0,1}s_{0,2}s_{1,0}s_{2,0}+(1-4g+g^2)s_{0,3}s_{1,0}s_{2,0} \\ +(-9+5g-g^2)s_{0,1}^2s_{1,1}s_{2,0}+(-26+27g-9g^2+g^3)s_{0,2}s_{1,1}s_{2,0} \\ +(23-16g+3g^2)s_{0,1}s_{1,2}s_{2,0}+(12-16g+7g^2-g^3)s_{1,3}s_{2,0}]$$

$$\begin{aligned}
& + (7-5g)s_{0,1}^2 s_{1,0} s_{2,1} + (23-16g+3g^2)s_{0,2} s_{1,0} s_{2,1} \\
& + (6-4g+2g^2)s_{0,1} s_{1,1} s_{2,1} + (-36+25g-5g^2)s_{1,2} s_{2,1} \\
& + (-26+11g+g^2)s_{0,1} s_{1,0} s_{2,2} + (36-28g+7g^2-g^3)s_{1,1} s_{2,2} \\
& + (-12+18g-6g^2)s_{1,0} s_{2,3} + (3-g)s_{0,1}^3 s_{3,0} + (1-4g+g^2)s_{0,1} s_{0,2} s_{3,0} \\
& + (-4+5g-g^2)s_{0,3} s_{3,0} + (-2-g+g^2)s_{0,1}^2 s_{3,1} + (12-16g+7g^2-g^3)s_{0,2} s_{3,1} \\
& + (-12+18g-6g^2)s_{0,1} s_{3,2} + (4g-6g^2+2g^3)s_{3,3} \big] \tag{A.18}
\end{aligned}$$

$$\begin{aligned}
\widehat{\mu_{1,3}\mu_{2,0}} = & \frac{1}{(g-5)(g-4)(g-3)(g-2)(g-1)g} \big[ 3s_{0,1}^3 s_{1,0}^3 + (6-3g)s_{0,1} s_{0,2} s_{1,0}^3 \\
& + (11-6g+g^2)s_{0,3} s_{1,0}^3 + (-12-3g)s_{0,1}^2 s_{1,0}^2 s_{1,1} + (-33+12g)s_{0,2} s_{1,0}^2 s_{1,1} \\
& + (-6+12g)s_{0,1} s_{1,0} s_{1,1}^2 + (12-6g)s_{1,1}^3 + (39-12g+3g^2)s_{0,1} s_{1,0}^2 s_{1,2} \\
& + (-18+12g-6g^2)s_{1,0} s_{1,1} s_{1,2} + (6-17g+6g^2-g^3)s_{1,0}^2 s_{1,3} \\
& + (6-3g)s_{0,1}^3 s_{1,0} s_{2,0} + (-3-9g+3g^2)s_{0,1} s_{0,2} s_{1,0} s_{2,0} \\
& + (-3-8g+6g^2-g^3)s_{0,3} s_{1,0} s_{2,0} + (27-15g+3g^2)s_{0,1}^2 s_{1,1} s_{2,0} \\
& + (-42+33g-6g^2)s_{0,2} s_{1,1} s_{2,0} + (51-66g+24g^2-3g^3)s_{0,1} s_{1,2} s_{2,0} \\
& + (24-39g+29g^2-9g^3+g^4)s_{1,3} s_{2,0} + (-21+15g)s_{0,1}^2 s_{1,0} s_{2,1} \\
& + (51-6g-3g^2)s_{0,2} s_{1,0} s_{2,1} + (-18+12g-6g^2)s_{0,1} s_{1,1} s_{2,1} \\
& + (-72+66g-21g^2+3g^3)s_{1,2} s_{2,1} + (-42+21g-9g^2)s_{0,1} s_{1,0} s_{2,2} \\
& + (72-57g+15g^2)s_{1,1} s_{2,2} + (-24+33g-12g^2+3g^3)s_{1,0} s_{2,3} \\
& + (-9+3g)s_{0,1}^3 s_{3,0} + (-3+12g-3g^2)s_{0,1} s_{0,2} s_{3,0} \\
& + (-8+14g-7g^2+g^3)s_{0,3} s_{3,0} + (6+3g-3g^2)s_{0,1}^2 s_{3,1} \\
& + (24-39g+9g^2)s_{0,2} s_{3,1} + (-24+33g-12g^2+3g^3)s_{0,1} s_{3,2} \\
& + (8g-11g^2+4g^3-g^4)s_{3,3} \big] \tag{A.19}
\end{aligned}$$

$$\widehat{\mu_{0,2}\mu_{3,1}} = \widehat{\mu_{1,3}\mu_{2,0}}^{(\text{sym})} \tag{A.20}$$

$$\begin{aligned}
\widehat{\mu_{1,2}\mu_{2,1}} = & \frac{1}{(g-5)(g-4)(g-3)(g-2)(g-1)g} \big[ 4s_{0,1}^3 s_{1,0}^3 + (-2-2g)s_{0,1} s_{0,2} s_{1,0}^3 + (-2+2g)s_{0,3} s_{1,0}^3 \\
& + (4-8g)s_{0,1}^2 s_{1,0}^2 s_{1,1} + (6-4g+2g^2)s_{0,2} s_{1,0}^2 s_{1,1} \\
& + (-8-4g+4g^2)s_{0,1} s_{1,0} s_{1,1}^2 + (-24+20g-4g^2)s_{1,1}^3 \\
& + (2+4g+2g^2)s_{0,1} s_{1,0}^2 s_{1,2} + (36-26g+8g^2-2g^3)s_{1,0} s_{1,1} s_{1,2} \\
& + (-12+8g-4g^2)s_{1,0}^2 s_{1,3} + (-2-2g)s_{0,1}^3 s_{1,0} s_{2,0} \\
& + (-4+3g+g^2)s_{0,1} s_{0,2} s_{1,0} s_{2,0} + (6-g-g^2)s_{0,3} s_{1,0} s_{2,0} \\
& + (6-4g+2g^2)s_{0,1}^2 s_{1,1} s_{2,0} + (-36+25g-5g^2)s_{0,2} s_{1,1} s_{2,0} \\
& + (18-18g+5g^2-g^3)s_{0,1} s_{1,2} s_{2,0} + (12-3g-2g^2+g^3)s_{1,3} s_{2,0} \\
& + (2+4g+2g^2)s_{0,1}^2 s_{1,0} s_{2,1} + (18-18g+5g^2-g^3)s_{0,2} s_{1,0} s_{2,1} \\
& + (36-26g+8g^2-2g^3)s_{0,1} s_{1,1} s_{2,1} + (-36-9g+24g^2-8g^3+g^4)s_{1,2} s_{2,1} \\
& + (-36+29g-13g^2)s_{0,1} s_{1,0} s_{2,2} + (36-9g-11g^2+4g^3)s_{1,1} s_{2,2} \\
& + (-12+15g-6g^2+3g^3)s_{1,0} s_{2,3} + (-2+2g)s_{0,1}^3 s_{3,0} \\
& + (6-g-g^2)s_{0,1} s_{0,2} s_{3,0} + (-4-g+g^2)s_{0,3} s_{3,0} \\
& + (-12+8g-4g^2)s_{0,1}^2 s_{3,1} + (12-3g-2g^2+g^3)s_{0,2} s_{3,1} \\
& + (-12+15g-6g^2+3g^3)s_{0,1} s_{3,2} + (4g-5g^2+2g^3-g^4)s_{3,3} \big] \tag{A.21}
\end{aligned}$$

$$\begin{aligned}
\widehat{\mu_{1,1}\mu_{2,2}} = & \frac{1}{(g-5)(g-4)(g-3)(g-2)(g-1)g} \big[ 3s_{0,1}^3 s_{1,0}^3 + (-4-g)s_{0,1} s_{0,2} s_{1,0}^3 \\
& + (1+g)s_{0,3} s_{1,0}^3 + (8-7g)s_{0,1}^2 s_{1,0}^2 s_{1,1} + (-3+g+g^2)s_{0,2} s_{1,0}^2 s_{1,1} \\
& + (-6-8g+4g^2)s_{0,1} s_{1,0} s_{1,1}^2 + (-28+22g-4g^2)s_{1,1}^3 + (9-g+2g^2)s_{0,1} s_{1,0}^2 s_{1,2} \\
& + (42-30g+10g^2-2g^3)s_{1,0} s_{1,1} s_{1,2} + (-14+7g-3g^2)s_{1,0}^2 s_{1,3} + (-4-g)s_{0,1}^3 s_{1,0} s_{2,0} \\
& + (-3+6g)s_{0,1} s_{0,2} s_{1,0} s_{2,0} + (7-5g)s_{0,3} s_{1,0} s_{2,0} + (-3+g+g^2)s_{0,1}^2 s_{1,1} s_{2,0} \\
& + (-2+5g-2g^2)s_{0,2} s_{1,1} s_{2,0} + (-19+13g-4g^2)s_{0,1} s_{1,2} s_{2,0} + (24-19g+5g^2)s_{1,3} s_{2,0} \\
& + (9-g+2g^2)s_{0,1}^2 s_{1,0} s_{2,1} + (-19+13g-4g^2)s_{0,2} s_{1,0} s_{2,1} + (42-30g+10g^2-2g^3)s_{0,1} s_{1,1} s_{2,1} \\
& + (-72+76g-28g^2+4g^3)s_{1,2} s_{2,1} + (-2-7g-g^3)s_{0,1} s_{1,0} s_{2,2} \\
& + (72-97g+43g^2-9g^3+g^4)s_{1,1} s_{2,2} + (-24+33g-12g^2+3g^3)s_{1,0} s_{2,3} + \\
& + (1+g)s_{0,1}^3 s_{3,0} + (7-5g)s_{0,1} s_{0,2} s_{3,0} + (-8+4g)s_{0,3} s_{3,0} \big]
\end{aligned}$$

$$+ (-14 + 7g - 3g^2)s_{0,1}^2s_{3,1} + (24 - 19g + 5g^2)s_{0,2}s_{3,1} + (-24 + 33g - 12g^2 + 3g^3)s_{0,1}s_{3,2} \\ + (8g - 11g^2 + 4g^3 - g^4)s_{3,3}] \quad (\text{A.22})$$

$$\widehat{\mu_{0,3}\mu_{3,0}} = \frac{1}{(-5+g)(-4+g)(-3+g)(-2+g)(-1+g)g} [ \\ 4s_{0,1}^3s_{1,0}^3 + (18-6g)s_{0,1}s_{0,2}s_{1,0}^3 + (18-12g+2g^2)s_{0,3}s_{1,0}^3 \\ - 36s_{0,1}^2s_{1,0}^2s_{1,1} + (-54+18g)s_{0,2}s_{1,0}^2s_{1,1} + 72s_{0,1}s_{1,0}s_{1,1}^2 \\ - 24s_{1,1}^3 + (-18+18g)s_{0,1}s_{1,0}^2s_{1,2} + (36-36g)s_{1,0}s_{1,1}s_{1,2} \\ + (-12+18g-6g^2)s_{1,0}^2s_{1,3} + (18-6g)s_{0,1}^3s_{1,0}s_{2,0} \\ + (36-45g+9g^2)s_{0,1}s_{0,2}s_{1,0}s_{2,0} + (6-36g+21g^2-3g^3)s_{0,3}s_{1,0}s_{2,0} \\ + (-54+18g)s_{0,1}^2s_{1,1}s_{2,0} + (-36+45g-9g^2)s_{0,2}s_{1,1}s_{2,0} \\ + (18+27g-9g^2)s_{0,1}s_{1,2}s_{2,0} + (12-3g-12g^2+3g^3)s_{1,3}s_{2,0} \\ + (-18+18g)s_{0,1}^2s_{1,0}s_{2,1} + (18+27g-9g^2)s_{0,2}s_{1,0}s_{2,1} \\ + (36-36g)s_{0,1}s_{1,1}s_{2,1} + (-36-9g+9g^2)s_{1,2}s_{2,1} \\ + (-36+9g-9g^2)s_{0,1}s_{1,0}s_{2,2} + (36-9g+9g^2)s_{1,1}s_{2,2} \\ + (-12+15g-6g^2+3g^3)s_{1,0}s_{2,3} + (18-12g+2g^2)s_{0,1}^3s_{3,0} \\ + (6-36g+21g^2-3g^3)s_{0,1}s_{0,2}s_{3,0} + (-4-g+16g^2-8g^3+g^4)s_{0,3}s_{3,0} \\ + (-12+18g-6g^2)s_{0,1}^2s_{3,1} + (12-3g-12g^2+3g^3)s_{0,2}s_{3,1} \\ + (-12+15g-6g^2+3g^3)s_{0,1}s_{3,2} + (4g-5g^2+2g^3-g^4)s_{3,3}] \quad (\text{A.23})$$

## Appendix B. Variance and covariance terms used in the Control Variates estimators

This appendix provides the explicit definitions of the variance and covariance terms appearing in the quadratic forms of the Control Variates estimators introduced in Sections 3.2–3.4. Throughout this appendix,  $\widehat{\sigma}^2[\cdot]$  denotes the sample variance of an estimator,  $\widehat{\text{Cov}}[\cdot, \cdot]$  denotes the sample covariance between two estimators, and  $g$  denotes the sample size, which can be either  $n$  or  $m_\ell$ ,  $\ell = 1, \dots, L$ .

It is important to note that the definitions presented in this appendix correspond to the case of Control Variates without Splitting, where the sample sets are used as a whole (i.e., without subdivision). When the Splitting scheme is applied, the same definitions remain valid but must be interpreted at the subset level, that is, evaluated with  $\theta_{n^*,j}$  and  $\theta_{m_\ell^*,j}$  for  $j = 1, 2, 3$  and  $\ell = 1, \dots, L$ .

### B.1. Mean estimator

The first set of terms, denoted by  $A_1$ – $A_4$ , correspond to the variance and covariance components appearing in the quadratic form of the Control Variates estimator of the mean. Their definitions are provided below:

$$A_1(r; \theta_n) := \widehat{\sigma}^2[\widehat{\mu}_1^T(r; \theta_n)], \quad (\text{B.1})$$

$$A_2(r, \tilde{r}; \theta_n) = \begin{pmatrix} A_{2,(1)} \\ A_{2,(2)} \\ \vdots \\ A_{2,(L)} \end{pmatrix}, \\ A_{2,(\ell)}(r, \tilde{r}; \theta_n) := \widehat{\text{Cov}}[\widehat{\mu}_1^T(r; \theta_n), \widehat{\mu}_1^T(\tilde{r}_\ell; \theta_n)], \quad \ell = 1, \dots, L, \quad (\text{B.2})$$

$$A_3(\tilde{r}; \theta_n) = \begin{pmatrix} A_{3,(1,1)} & A_{3,(1,2)} & \cdots & A_{3,(1,L)} \\ A_{3,(2,1)} & A_{3,(2,2)} & \cdots & A_{3,(2,L)} \\ \vdots & \vdots & \ddots & \vdots \\ A_{3,(L,1)} & A_{3,(L,2)} & \cdots & A_{3,(L,L)} \end{pmatrix}, \\ A_{3,(\ell_1, \ell_2)}(\tilde{r}; \theta_n) := \begin{cases} \widehat{\text{Cov}}[\widehat{\mu}_1^T(\tilde{r}_{\ell_1}; \theta_n), \widehat{\mu}_1^T(\tilde{r}_{\ell_2}; \theta_n)], & \ell_1 \neq \ell_2, \\ \widehat{\sigma}^2[\widehat{\mu}_1^T(\tilde{r}_{\ell_1}; \theta_n)], & \ell_1 = \ell_2, \end{cases} \quad \ell_1, \ell_2 = 1, \dots, L, \quad (\text{B.3})$$

$$A_4(\tilde{r}; \theta_m) = \begin{pmatrix} A_{4,(1)} & 0 & \cdots & 0 \\ 0 & A_{4,(2)} & \cdots & 0 \\ \vdots & \vdots & \ddots & \vdots \\ 0 & 0 & \cdots & A_{4,(L)} \end{pmatrix}, \\ A_{4,(\ell)}(\tilde{r}; \theta_{m_\ell}) := \widehat{\sigma}^2[\widehat{\mu}_1^T(\tilde{r}_\ell; \theta_{m_\ell})], \quad \ell = 1, \dots, L. \quad (\text{B.4})$$



The variances and covariances appearing in the definitions of  $A_1$ – $A_4$  (see Eqs. (B.1)–(B.4)) are computed using the following explicit formulas for the variance of the first-order moment estimator of a single model response  $y$ , and for the covariance between the first-order moment estimators of two model responses  $y_a$  and  $y_b$ :

$$\hat{\sigma}^2[\hat{\mu}_1'(y; \boldsymbol{\theta}_g)] = \frac{\hat{\mu}_2(y; \boldsymbol{\theta}_g)}{g}, \quad (\text{B.5})$$

$$\widehat{\text{Cov}}[\hat{\mu}_1'(y_a; \boldsymbol{\theta}_g), \hat{\mu}_1'(y_b; \boldsymbol{\theta}_g)] = \frac{\hat{\mu}_{1,1}(y_a, y_b; \boldsymbol{\theta}_g)}{g}. \quad (\text{B.6})$$

Formulas for calculating the moments and co-moments appearing in Eqs. (B.5) and (B.6) are provided in [Appendix A](#).

### B.2. Variance estimator

The terms  $B_1$ – $B_4$  define the variance and covariance components appearing in the quadratic form of the Control Variates estimator of the variance. Their definitions are given below:

$$B_1(r; \boldsymbol{\theta}_n) := \hat{\sigma}^2[\hat{\mu}_2(r; \boldsymbol{\theta}_n)], \quad (\text{B.7})$$

$$B_2(r, \tilde{r}; \boldsymbol{\theta}_n) = \begin{pmatrix} B_{2,(1)} \\ B_{2,(2)} \\ \vdots \\ B_{2,(L)} \end{pmatrix},$$

$$B_{2,(\ell)}(r, \tilde{r}; \boldsymbol{\theta}_n) := \widehat{\text{Cov}}[\hat{\mu}_2(r; \boldsymbol{\theta}_n), \hat{\mu}_2(\tilde{r}; \boldsymbol{\theta}_n)], \quad \ell = 1, \dots, L, \quad (\text{B.8})$$

$$B_3(\tilde{r}; \boldsymbol{\theta}_n) = \begin{pmatrix} B_{3,(1,1)} & B_{3,(1,2)} & \cdots & B_{3,(1,L)} \\ B_{3,(2,1)} & B_{3,(2,2)} & \cdots & B_{3,(2,L)} \\ \vdots & \vdots & \ddots & \vdots \\ B_{3,(L,1)} & B_{3,(L,2)} & \cdots & B_{3,(L,L)} \end{pmatrix},$$

$$B_{3,(\ell_1, \ell_2)}(\tilde{r}; \boldsymbol{\theta}_n) := \begin{cases} \widehat{\text{Cov}}[\hat{\mu}_2(\tilde{r}_{\ell_1}; \boldsymbol{\theta}_n), \hat{\mu}_2(\tilde{r}_{\ell_2}; \boldsymbol{\theta}_n)], & \ell_1 \neq \ell_2, \\ \hat{\sigma}^2[\hat{\mu}_2(\tilde{r}_{\ell_1}; \boldsymbol{\theta}_n)], & \ell_1 = \ell_2, \end{cases} \quad \ell_1, \ell_2 = 1, \dots, L, \quad (\text{B.9})$$

$$B_4(\tilde{r}; \boldsymbol{\theta}_m) = \begin{pmatrix} B_{4,(1)} & 0 & \cdots & 0 \\ 0 & B_{4,(2)} & \cdots & 0 \\ \vdots & \vdots & \ddots & \vdots \\ 0 & 0 & \cdots & B_{4,(L)} \end{pmatrix},$$

$$B_{4,(\ell)}(\tilde{r}; \boldsymbol{\theta}_{m_\ell}) := \hat{\sigma}^2[\hat{\mu}_2(\tilde{r}_\ell; \boldsymbol{\theta}_{m_\ell})], \quad \ell = 1, \dots, L. \quad (\text{B.10})$$

The variances and covariances appearing in the definitions of  $B_1$ – $B_4$  (Eqs. (B.7)–(B.10)) are computed using the following explicit formulas for the variance of a second-order moment estimator of a single model response  $y$ , and for the covariance between the second-order moment estimators of two model responses  $y_a$  and  $y_b$ :

$$\hat{\sigma}^2[\hat{\mu}_2(y; \boldsymbol{\theta}_g)] = \frac{\hat{\mu}_4(y; \boldsymbol{\theta}_g)}{g} - \frac{(g-3)}{(g-1)g} \hat{\mu}_2^2(y; \boldsymbol{\theta}_g), \quad (\text{B.11})$$

$$\begin{aligned} \widehat{\text{Cov}}[\hat{\mu}_2(y_a; \boldsymbol{\theta}_g), \hat{\mu}_2(y_b; \boldsymbol{\theta}_g)] &= \frac{2}{(g-1)g} \hat{\mu}_{1,1}^2(y_a, y_b; \boldsymbol{\theta}_g) + \frac{1}{g} \hat{\mu}_{2,2}(y_a, y_b; \boldsymbol{\theta}_g) \\ &\quad - \frac{1}{g} \hat{\mu}_{2,0} \hat{\mu}_{0,2}(y_a, y_b; \boldsymbol{\theta}_g). \end{aligned} \quad (\text{B.12})$$

Formulas for calculating the moments, co-moments, and their squared and product terms appearing in Eqs. (B.11) and (B.12) can be found in [Appendix A](#).

### B.3. Third-order moment estimator

The terms  $C_1$ – $C_4$  define the variance and covariance components appearing in the quadratic form of the Control Variates estimator of the third central moment. Their definitions are given below:

$$C_1(r; \boldsymbol{\theta}_n) := \hat{\sigma}^2[\hat{\mu}_3(r; \boldsymbol{\theta}_n)], \quad (\text{B.13})$$

$$C_2(r, \tilde{r}; \boldsymbol{\theta}_n) = \begin{pmatrix} C_{2,(1)} \\ C_{2,(2)} \\ \vdots \\ C_{2,(L)} \end{pmatrix},$$

$$C_{2,(\ell)}(r, \tilde{r}; \boldsymbol{\theta}_n) := \widehat{\text{Cov}}[\hat{\mu}_3(r; \boldsymbol{\theta}_n), \hat{\mu}_3(\tilde{r}_\ell; \boldsymbol{\theta}_n)], \quad \ell = 1, \dots, L, \quad (\text{B.14})$$

$$C_3(\tilde{\mathbf{r}}; \boldsymbol{\theta}_n) = \begin{pmatrix} C_{3,(1,1)} & C_{3,(1,2)} & \cdots & C_{3,(1,L)} \\ C_{3,(2,1)} & C_{3,(2,2)} & \cdots & C_{3,(2,L)} \\ \vdots & \vdots & \ddots & \vdots \\ C_{3,(L,1)} & C_{3,(L,2)} & \cdots & C_{3,(L,L)} \end{pmatrix}, \quad (\text{B.15})$$

$$C_{3,(\ell_1, \ell_2)}(\tilde{\mathbf{r}}; \boldsymbol{\theta}_n) := \begin{cases} \widehat{\text{Cov}}[\widehat{\mu}_3(\tilde{\mathbf{r}}_{\ell_1}; \boldsymbol{\theta}_n), \widehat{\mu}_3(\tilde{\mathbf{r}}_{\ell_2}; \boldsymbol{\theta}_n)], & \ell_1 \neq \ell_2, \\ \widehat{\sigma}^2[\widehat{\mu}_3(\tilde{\mathbf{r}}_{\ell_1}; \boldsymbol{\theta}_n)], & \ell_1 = \ell_2, \end{cases} \quad \ell_1, \ell_2 = 1, \dots, L,$$

$$C_4(\tilde{\mathbf{r}}; \boldsymbol{\theta}_m) = \begin{pmatrix} C_{4,(1)} & 0 & \cdots & 0 \\ 0 & C_{4,(2)} & \cdots & 0 \\ \vdots & \vdots & \ddots & \vdots \\ 0 & 0 & \cdots & C_{4,(L)} \end{pmatrix}, \quad (\text{B.16})$$

$$C_{4,(\ell)}(\tilde{\mathbf{r}}; \boldsymbol{\theta}_{m_\ell}) := \widehat{\sigma}^2[\widehat{\mu}_3(\tilde{\mathbf{r}}_\ell; \boldsymbol{\theta}_{m_\ell})], \quad \ell = 1, \dots, L.$$

The variances and covariances appearing in the definitions of  $C_1$ – $C_4$  (Eqs. (B.13)–(B.16)) are computed using the following explicit formulas for the variance of a third-order moment estimator of a single model response  $y$ , and for the covariance between the third-order moment estimators of two model responses  $y_a$  and  $y_b$ :

$$\begin{aligned} \widehat{\sigma}^2[\widehat{\mu}_3(y; \boldsymbol{\theta}_g)] &= \frac{3(20 - 12g + 3g^2)}{(g-2)(g-1)g} \widehat{\mu}_2^3(y; \boldsymbol{\theta}_g) - \frac{(g-10)}{(g-1)g} \widehat{\mu}_3^2(y; \boldsymbol{\theta}_g) \\ &\quad - \frac{3(2g-5)}{(g-1)g} \widehat{\mu}_2 \widehat{\mu}_4(y; \boldsymbol{\theta}_g) + \frac{1}{g} \widehat{\mu}_6(y; \boldsymbol{\theta}_g), \\ \widehat{\text{Cov}}[\widehat{\mu}_3(y_a; \boldsymbol{\theta}_g), \widehat{\mu}_3(y_b; \boldsymbol{\theta}_g)] &= \frac{24}{(g-2)(g-1)g} \widehat{\mu}_{1,1}^3(y_a, y_b; \boldsymbol{\theta}_g) \\ &\quad + \frac{9(g-2)}{(g-1)g} \widehat{\mu}_{0,2} \widehat{\mu}_{1,1} \widehat{\mu}_{2,0}(y_a, y_b; \boldsymbol{\theta}_g) \\ &\quad - \frac{3}{g} \widehat{\mu}_{1,3} \widehat{\mu}_{2,0}(y_a, y_b; \boldsymbol{\theta}_g) \\ &\quad + \frac{9}{(g-1)g} \widehat{\mu}_{1,2} \widehat{\mu}_{2,1}(y_a, y_b; \boldsymbol{\theta}_g) \\ &\quad + \frac{9}{(g-1)g} \widehat{\mu}_{1,1} \widehat{\mu}_{2,2}(y_a, y_b; \boldsymbol{\theta}_g) \\ &\quad - \frac{1}{g} \widehat{\mu}_{0,3} \widehat{\mu}_{3,0}(y_a, y_b; \boldsymbol{\theta}_g) \\ &\quad - \frac{3}{g} \widehat{\mu}_{0,2} \widehat{\mu}_{3,1}(y_a, y_b; \boldsymbol{\theta}_g) + \frac{1}{g} \widehat{\mu}_{3,3}(y_a, y_b; \boldsymbol{\theta}_g). \end{aligned} \quad (\text{B.17})$$

Formulas for calculating the moments, co-moments, and their squared, cubed, and product terms appearing in Eqs. (B.17) and (B.18) can be found in [Appendix A](#).

### Appendix C. Origin of bias in Control Variates and its elimination by splitting

Let  $\mu$  denote any statistical moment of the response, and  $\beta$  the associated control parameter. The following derivation shows why the Control Variates (CV) estimator without Splitting is biased, and how this bias is eliminated by the Splitting technique.

#### Bias of CV without splitting

$$\widehat{\mu}^{\text{CV}} = \widehat{\mu}(r; \boldsymbol{\theta}_n) - \widehat{\beta}^{*\top} (\widehat{\mu}(\tilde{\mathbf{r}}; \boldsymbol{\theta}_n) - \widehat{\mu}(\tilde{\mathbf{r}}; \boldsymbol{\theta}_m)) \quad (\text{C.1})$$

The bias of this estimator is defined as:

$$\text{Bias}[\widehat{\mu}^{\text{CV}}] = \mathbb{E}[\widehat{\mu}^{\text{CV}}] - \mu(r) \quad (\text{C.2})$$

Substituting the definition of  $\widehat{\mu}^{\text{CV}}$ :

$$\text{Bias}[\widehat{\mu}^{\text{CV}}] = \mathbb{E}[\widehat{\mu}(r; \boldsymbol{\theta}_n)] - \mathbb{E}[\widehat{\beta}^{*\top} \widehat{\mu}(\tilde{\mathbf{r}}; \boldsymbol{\theta}_n)] + \mathbb{E}[\widehat{\beta}^{*\top} \widehat{\mu}(\tilde{\mathbf{r}}; \boldsymbol{\theta}_m)] - \mu(r) \quad (\text{C.3})$$

Using the identity  $\mathbb{E}[\mathbf{x}_1^\top \mathbf{x}_2] = \mathbb{E}[\mathbf{x}_1]^\top \mathbb{E}[\mathbf{x}_2] + \text{tr}(\text{Cov}(\mathbf{x}_1, \mathbf{x}_2))$ , where  $\text{tr}(\cdot)$  denotes the trace operator:

$$\begin{aligned} \text{Bias}[\widehat{\mu}^{\text{CV}}] &= \mu(r) - \mathbb{E}[\widehat{\beta}^{*\top}]^\top \mu(\tilde{\mathbf{r}}) - \text{tr}(\text{Cov}(\widehat{\beta}^*, \widehat{\mu}(\tilde{\mathbf{r}}; \boldsymbol{\theta}_n))) \\ &\quad + \mathbb{E}[\widehat{\beta}^{*\top}]^\top \mu(\tilde{\mathbf{r}}) + \text{tr}(\text{Cov}(\widehat{\beta}^*, \widehat{\mu}(\tilde{\mathbf{r}}; \boldsymbol{\theta}_m))) - \mu(r) \end{aligned} \quad (\text{C.4})$$

Simplifying the mean terms yields:

$$\text{Bias}[\widehat{\mu}^{\text{CV}}] = -\text{tr}(\text{Cov}(\widehat{\beta}^*, \widehat{\mu}(\tilde{\mathbf{r}}; \boldsymbol{\theta}_n))) + \text{tr}(\text{Cov}(\widehat{\beta}^*, \widehat{\mu}(\tilde{\mathbf{r}}; \boldsymbol{\theta}_m))) \quad (\text{C.5})$$

Let the vectors be written explicitly as:

$$\hat{\beta}^* = [\hat{\beta}^*(r, \tilde{r}_1; \boldsymbol{\theta}_n, \boldsymbol{\theta}_{m_1}), \dots, \hat{\beta}^*(r, \tilde{r}_L; \boldsymbol{\theta}_n, \boldsymbol{\theta}_{m_L})]^\top \quad (\text{C.6})$$

$$\hat{\mu}(\tilde{r}; \boldsymbol{\theta}_n) = [\hat{\mu}(\tilde{r}_1; \boldsymbol{\theta}_n), \dots, \hat{\mu}(\tilde{r}_L; \boldsymbol{\theta}_n)]^\top \quad (\text{C.7})$$

$$\hat{\mu}(\tilde{r}; \boldsymbol{\theta}_m) = [\hat{\mu}(\tilde{r}_1; \boldsymbol{\theta}_{m_1}), \dots, \hat{\mu}(\tilde{r}_L; \boldsymbol{\theta}_{m_L})]^\top \quad (\text{C.8})$$

Then, the bias expression can be rewritten as:

$$\begin{aligned} \text{Bias}[\hat{\mu}^{\text{CV}}] &= - \sum_{i=1}^L \text{Cov}(\hat{\beta}^*(r, \tilde{r}_i; \boldsymbol{\theta}_n, \boldsymbol{\theta}_{m_i}), \hat{\mu}(\tilde{r}_i; \boldsymbol{\theta}_n)) \\ &\quad + \sum_{i=1}^L \text{Cov}(\hat{\beta}^*(r, \tilde{r}_i; \boldsymbol{\theta}_n, \boldsymbol{\theta}_{m_i}), \hat{\mu}(\tilde{r}_i; \boldsymbol{\theta}_{m_i})) \end{aligned} \quad (\text{C.9})$$

The bias expression in (C.9) can be rearranged into a more compact form:

$$\text{Bias}[\hat{\mu}^{\text{CV}}] = \sum_{i=1}^L \text{Cov}(\hat{\beta}^*(r, \tilde{r}_i; \boldsymbol{\theta}_n, \boldsymbol{\theta}_{m_i}), \hat{\mu}(\tilde{r}_i; \boldsymbol{\theta}_{m_i}) - \hat{\mu}(\tilde{r}_i; \boldsymbol{\theta}_n)) \quad (\text{C.10})$$

Eq. (C.10) shows that the bias can vanish if the covariance terms are equal to zero. Two situations in which the covariance of two quantities vanishes are the following: (i) when at least one of them is constant, or (ii) when they are computed from disjoint sample sets.

Analyzing situation (i), it can be observed that the first quantity  $\hat{\beta}^*$ , and the second one  $(\hat{\mu}(\tilde{r}_i; \boldsymbol{\theta}_{m_i}) - \hat{\mu}(\tilde{r}_i; \boldsymbol{\theta}_n))$  are random variables, not constants. Even though the second quantity is a difference with zero mean, it fluctuates around zero, and covariance measures precisely the joint fluctuations around the means. Therefore, situation (i) does not apply.

Analyzing situation (ii), it can be seen that the estimators share the same sample sets, and are therefore correlated. Thus, situation (ii) does not apply either.

Consequently, the covariance terms are not zero, which implies that the Control Variates estimator is biased:

$$\text{Bias}[\hat{\mu}^{\text{CV}}] \neq 0 \quad (\text{C.11})$$

One way to force situation (i) is to make that the estimators converge to constants by letting  $n, m \rightarrow \infty$ . This corresponds to the definition of a biased but consistent estimator, which is precisely the case of the traditional Control Variates method. However, forcing convergence in this way is not practically feasible.

Another alternative is to force situation (ii) by computing the quantities from disjoint sample sets, which makes them uncorrelated and forces the covariance terms to vanish. This is precisely the idea behind the Splitting technique.

#### Bias of CV with splitting

$$\hat{\mu}^{\text{CV+S}} = \frac{1}{3} \sum_{j=1}^3 \left[ \hat{\mu}(r; \boldsymbol{\theta}_{n^*,j}) - \hat{\beta}_{\tau(j)}^* (\hat{\mu}(\tilde{r}; \boldsymbol{\theta}_{n^*,j}) - \hat{\mu}(\tilde{r}; \boldsymbol{\theta}_{m^*,j})) \right] \quad (\text{C.12})$$

The bias of this estimator is:

$$\text{Bias}[\hat{\mu}^{\text{CV+S}}] = \mathbb{E}[\hat{\mu}^{\text{CV+S}}] - \mu(r) \quad (\text{C.13})$$

Applying the same identity used before, each expectation of a product  $\hat{\beta}_{\tau(j)}^* \hat{\mu}(\cdot)$  is decomposed into mean terms and a trace of covariance. After simplification, the bias reads:

$$\begin{aligned} \text{Bias}[\hat{\mu}^{\text{CV+S}}] &= -\frac{1}{3} \sum_{j=1}^3 \text{tr}(\text{Cov}(\hat{\beta}_{\tau(j)}^*, \hat{\mu}(\tilde{r}; \boldsymbol{\theta}_{n^*,j}))) \\ &\quad + \frac{1}{3} \sum_{j=1}^3 \text{tr}(\text{Cov}(\hat{\beta}_{\tau(j)}^*, \hat{\mu}(\tilde{r}; \boldsymbol{\theta}_{m^*,j}))) \end{aligned} \quad (\text{C.14})$$

Writing explicitly the vectors for each subset  $j$ :

$$\hat{\beta}_{\tau(j)}^* = [\hat{\beta}^*(r, \tilde{r}_1; \boldsymbol{\theta}_{n^*,\tau(j)}, \boldsymbol{\theta}_{m_1^*,\tau(j)}), \dots, \hat{\beta}^*(r, \tilde{r}_L; \boldsymbol{\theta}_{n^*,\tau(j)}, \boldsymbol{\theta}_{m_L^*,\tau(j)})]^\top \quad (\text{C.15})$$

$$\hat{\mu}(\tilde{r}; \boldsymbol{\theta}_{n^*,j}) = [\hat{\mu}(\tilde{r}_1; \boldsymbol{\theta}_{n^*,j}), \dots, \hat{\mu}(\tilde{r}_L; \boldsymbol{\theta}_{n^*,j})]^\top \quad (\text{C.16})$$

$$\hat{\mu}(\tilde{r}; \boldsymbol{\theta}_{m^*,j}) = [\hat{\mu}(\tilde{r}_1; \boldsymbol{\theta}_{m_1^*,j}), \dots, \hat{\mu}(\tilde{r}_L; \boldsymbol{\theta}_{m_L^*,j})]^\top \quad (\text{C.17})$$

Each trace in Eq. (C.14) becomes a sum of covariances of the  $i$ th components:

$$\begin{aligned} \text{Bias}[\hat{\mu}^{\text{CV+S}}] &= -\frac{1}{3} \sum_{j=1}^3 \sum_{i=1}^L \text{Cov}(\hat{\beta}^*(r, \tilde{r}_i; \boldsymbol{\theta}_{n^*,\tau(j)}, \boldsymbol{\theta}_{m_i^*,\tau(j)}), \hat{\mu}(\tilde{r}_i; \boldsymbol{\theta}_{n^*,j})) \\ &\quad + \frac{1}{3} \sum_{j=1}^3 \sum_{i=1}^L \text{Cov}(\hat{\beta}^*(r, \tilde{r}_i; \boldsymbol{\theta}_{n^*,\tau(j)}, \boldsymbol{\theta}_{m_i^*,\tau(j)}), \hat{\mu}(\tilde{r}_i; \boldsymbol{\theta}_{m_i^*,j})) \end{aligned} \quad (\text{C.18})$$

Since the sample sets  $\boldsymbol{\theta}_{n^*,\tau(j)}$  and  $\boldsymbol{\theta}_{m_i^*,\tau(j)}$  used for  $\hat{\beta}^*$  are independent from the sample sets used for the estimators  $\hat{\mu}(\tilde{r}_i; \boldsymbol{\theta}_{n^*,j})$  and  $\hat{\mu}(\tilde{r}_i; \boldsymbol{\theta}_{m_i^*,j})$ , all covariance terms are zero. Therefore, the Control Variates estimator with Splitting is unbiased:

$$\text{Bias}[\hat{\mu}^{\text{CV+S}}] = 0 \quad (\text{C.19})$$

## Appendix D. Calculation of maximum coefficient of variation of estimators

The maximum coefficient of variation among the estimators of the first three moments of the response is defined as:

$$\delta^{CV+S}(r, \tilde{r}, \Theta_{n^{(k-1)}}, \Theta_{m^{(k-1)}}, n, m) = \max \left\{ \frac{\sqrt{\hat{\sigma}^2 \left[ \hat{\mu}_1^{CV+S}(r, \tilde{r}, \Theta_{n^{(k-1)}}, \Theta_{m^{(k-1)}}, n, m) \right]}}{\left| \hat{\mu}_1^{CV+S}(r, \tilde{r}, \Theta_{n^{(k-1)}}, \Theta_{m^{(k-1)}}, n, m) \right|}, \frac{\sqrt{\hat{\sigma}^2 \left[ \hat{\mu}_2^{CV+S}(r, \tilde{r}, \Theta_{n^{(k-1)}}, \Theta_{m^{(k-1)}}, n, m) \right]}}{\left| \hat{\mu}_2^{CV+S}(r, \tilde{r}, \Theta_{n^{(k-1)}}, \Theta_{m^{(k-1)}}, n, m) \right|}, \frac{\sqrt{\hat{\sigma}^2 \left[ \hat{\mu}_3^{CV+S}(r, \tilde{r}, \Theta_{n^{(k-1)}}, \Theta_{m^{(k-1)}}, n, m) \right]}}{\left| \hat{\mu}_3^{CV+S}(r, \tilde{r}, \Theta_{n^{(k-1)}}, \Theta_{m^{(k-1)}}, n, m) \right|} \right\}. \quad (D.1)$$

In this equation,  $\hat{\mu}_1^{CV+S}(\cdot)$  and  $\hat{\sigma}^2 \left[ \hat{\mu}_1^{CV+S}(\cdot) \right]$  are the estimators of the mean of the response and its variance, respectively. Likewise,  $\hat{\mu}_2^{CV+S}(\cdot)$  and  $\hat{\sigma}^2 \left[ \hat{\mu}_2^{CV+S}(\cdot) \right]$  are the estimators of the variance of the response and its variance, respectively. Finally,  $\hat{\mu}_3^{CV+S}(\cdot)$  and  $\hat{\sigma}^2 \left[ \hat{\mu}_3^{CV+S}(\cdot) \right]$  are the estimators of the third central moment of the response and its variance. All six estimators are evaluated considering sample set sizes  $(n, m)$ , but the corresponding co-moments are computed using the sample sets  $(\Theta_{n^{(k-1)}}, \Theta_{m^{(k-1)}})$  from the previous iteration.

## Data availability

No data was used for the research described in the article.

## References

- [1] Bathe K. *Finite element procedures*. New Jersey: Prentice Hall; 1996.
- [2] Faes M, Moens D. Recent trends in the modeling and quantification of non-probabilistic uncertainty. *Arch Comput Methods Eng* 2020;27(3):633–71. <http://dx.doi.org/10.1007/s11831-019-09327-x>.
- [3] Ang A, Tang W. *Probability concepts in engineering: emphasis on applications to civil and environmental engineering*. Wiley; 2007.
- [4] Faes M, Broggi M, Spanos P, Beer M. Elucidating appealing features of differentiable auto-correlation functions: A study on the modified exponential kernel. *Probabilistic Eng Mech* 2022;69:103269. <http://dx.doi.org/10.1016/j.probengmech.2022.103269>, <https://www.sciencedirect.com/science/article/pii/S026689202200042X>.
- [5] Yamazaki F, Shinozuka M, Dasgupta G. Neumann expansion for stochastic finite element analysis. *J Eng Mech* 1988;114(8):1335–54. [http://dx.doi.org/10.1061/\(ASCE\)0733-9399\(1988\)114:8\(1335\)](http://dx.doi.org/10.1061/(ASCE)0733-9399(1988)114:8(1335)).
- [6] Li J, Chen J. Probability density evolution method for dynamic response analysis of structures with uncertain parameters. *Comput Mech* 2004;34(5):400–9. <http://dx.doi.org/10.1007/s00466-004-0583-8>.
- [7] Schueller G, Pradlwarter H, Koutsourelakis P. A critical appraisal of reliability estimation procedures for high dimensions. *Probabilistic Eng Mech* 2004;19(4):463–74.
- [8] Elishakoff I, Ren Y, Shinozuka M. Improved finite element method for stochastic problems. *Chaos Solitons Fractals* 1995;5(5):833–46. [http://dx.doi.org/10.1016/0960-0779\(94\)00157-L](http://dx.doi.org/10.1016/0960-0779(94)00157-L), <http://www.sciencedirect.com/science/article/pii/S096007799400157L>.
- [9] Fuchs M, Shabtay E. The reciprocal approximation in stochastic analysis of structures. *Chaos Solitons Fractals* 2000;11(6):889–900.
- [10] Hohenbichler M, Rackwitz R. First-order concepts in system reliability. *Struct Saf* 1983;1(3):177–88.
- [11] Adhikari S. Reliability analysis using parabolic failure surface approximation. *J Eng Mech* 2004;130(12):1407–27.
- [12] Chen G, Yang D. Direct probability integral method for stochastic response analysis of static and dynamic structural systems. *Comput Methods Appl Mech Engrg* 2019;357:112612. <http://dx.doi.org/10.1016/j.cma.2019.112612>, <http://www.sciencedirect.com/science/article/pii/S0045782519304888>.
- [13] Kougioumtzoglou I, Fragkoulis V, Pantelous A, Pirrotta A. Random vibration of linear and nonlinear structural systems with singular matrices: A frequency domain approach. *J Sound Vib* 2017;404:84–101. <http://dx.doi.org/10.1016/j.jsv.2017.05.038>, <http://www.sciencedirect.com/science/article/pii/S0022460X17304340>.
- [14] Li J, Chen J-B. The probability density evolution method for dynamic response analysis of non-linear stochastic structures. *Internat J Numer Methods Engrg* 2006;65(6):882–903. <http://dx.doi.org/10.1002/nme.1479>, <https://onlinelibrary.wiley.com/doi/pdf/10.1002/nme.1479>, <https://onlinelibrary.wiley.com/doi/abs/10.1002/nme.1479>.
- [15] Blatman G, Sudret B. An adaptive algorithm to build up sparse polynomial chaos expansions for stochastic finite element analysis. *Probabilistic Eng Mech* 2010;25(2):183–97. <http://dx.doi.org/10.1016/j.probengmech.2009.10.003>, <http://www.sciencedirect.com/science/article/pii/S0266892009000666>.
- [16] Echard B, Gayton N, Lemaire M. AK-MCS: An active learning reliability method combining kriging and Monte Carlo simulation. *Struct Saf* 2011;33(2):145–54. <http://dx.doi.org/10.1016/j.strusafe.2011.01.002>, <http://www.sciencedirect.com/science/article/pii/S0167473011000038>.
- [17] Su M, Wang Z, Bursi OS, Broccardo M. Surrogate modeling for probability distribution estimation: Uniform or adaptive design? *Reliab Eng Syst Saf* 2025;261:111059. <http://dx.doi.org/10.1016/j.res.2025.111059>.
- [18] Au S, Beck J. Estimation of small failure probabilities in high dimensions by subset simulation. *Probabilistic Eng Mech* 2001;16(4):263–77.
- [19] Papaioannou I, Papadimitriou C, Straub D. Sequential importance sampling for structural reliability analysis. *Struct Saf* 2016;62:66–75. <http://dx.doi.org/10.1016/j.strusafe.2016.06.002>, <http://www.sciencedirect.com/science/article/pii/S0167473016300169>.
- [20] Amsallem D, Cortial J, Carlberg K, Farhat C. A method for interpolating on manifolds structural dynamics reduced-order models. *Internat J Numer Methods Engrg* 2009;80(9):1241–58. <http://dx.doi.org/10.1002/nme.2681>.
- [21] Cao B-T, Freitag S, Meschke G. A hybrid RNN-GPOD surrogate model for real-time settlement predictions in mechanised tunnelling. *Adv Model Simul Eng Sci* 2016;3(5). <http://dx.doi.org/10.1186/s40323-016-0057-9>.
- [22] Chinesta F, Keunings R, Leygue A. *The proper generalized decomposition for advanced numerical simulations: a primer*. Springer Science & Business Media; 2013.
- [23] Farcaş IG, Peherstorfer B, Neckel T, Jenko F, Bungartz H-J. Context-aware learning of hierarchies of low-fidelity models for multifidelity uncertainty quantification. *Comput Methods Appl Mech Engrg* 2023;406:115908. <http://dx.doi.org/10.1016/j.cma.2023.115908>.
- [24] Blonigan PJ, Geraci G, Rizzi F, Eldred MS. Towards an integrated and efficient framework for leveraging reduced order models for multifidelity uncertainty quantification. In: *AIAA scitech 2020 forum*. American Institute of Aeronautics and Astronautics; 2020. <http://dx.doi.org/10.2514/6.2020-0420>.
- [25] Kennedy MC, O'Hagan A. Predicting the output from a complex computer code when fast approximations are available. *Biometrika* 2000;87(1):1–13. <http://dx.doi.org/10.1093/biomet/87.1.1>, <http://www.jstor.org/stable/2673557>.
- [26] Le Gratiet L, Garnier J. Recursive co-kriging model for design of computer experiments with multiple levels of fidelity. *Int J Uncertain Quantif* 2014;4(5):365–86. <http://dx.doi.org/10.1615/Int.J.UncertainQuantification.2014006914>.
- [27] Che Y, Ma Y, Chen H, Ma Y. Multi-fidelity kriging structural reliability analysis with the fusion of non-hierarchical low-fidelity models. *Reliab Eng Syst Saf* 2026;266:111662. <http://dx.doi.org/10.1016/j.res.2025.111662>, <https://www.sciencedirect.com/science/article/pii/S0951832025008622>.
- [28] Palar PS, Zuhail LR, Shimoyama K, Tsuchiya T. Global sensitivity analysis via multi-fidelity polynomial chaos expansion. *Reliab Eng Syst Saf* 2018;170:175–90. <http://dx.doi.org/10.1016/j.res.2017.10.013>, <https://www.sciencedirect.com/science/article/pii/S0951832016304872>.
- [29] Yan L, Zhou T. Adaptive multi-fidelity polynomial chaos approach to Bayesian inference in inverse problems. *J Comput Phys* 2019;381:110–28. <http://dx.doi.org/10.1016/j.jcp.2018.12.025>, <https://www.sciencedirect.com/science/article/pii/S0021999119300063>.



- [30] Karimi MS, Mohammadi R, Raisee M. Bi-fidelity adaptive sparse reconstruction of polynomial chaos using Bayesian compressive sensing. *Eng Comput* 2025. <http://dx.doi.org/10.1007/s00366-025-02112-4>.
- [31] Peherstorfer B, Cui T, Marzouk Y, Willcox K. Multifidelity importance sampling. *Comput Methods Appl Mech Engrg* 2016;300:490–509. <http://dx.doi.org/10.1016/j.cma.2015.12.002>, <https://www.sciencedirect.com/science/article/pii/S004578251500393X>.
- [32] Kramer B, Marques AN, Peherstorfer B, Villa U, Willcox K. Multifidelity probability estimation via fusion of estimators. *J Comput Phys* 2019;392:385–402. <http://dx.doi.org/10.1016/j.jcp.2019.04.071>, <https://www.sciencedirect.com/science/article/pii/S0021999119303249>.
- [33] Chakraborty P, Dhulipala SLN, Shields MD. Covariance-free bifidelity control variates importance sampling for rare event reliability analysis. *SIAM/ASA J Uncertain Quantif* 2025;13(3):1406–51. <http://dx.doi.org/10.1137/24M1658498>.
- [34] Lima JPS, Evangelista F, Guedes Soares C. Hyperparameter-optimized multifidelity deep neural network model associated with subset simulation for structural reliability analysis. *Reliab Eng Syst Saf* 2023;239:109492. <http://dx.doi.org/10.1016/j.res.2023.109492>, <https://www.sciencedirect.com/science/article/pii/S0951832023004064>.
- [35] Davis O, Motamed M, Tempone R. Residual multi-fidelity neural network computing. *BIT Numer Math* 2025;65(2). <http://dx.doi.org/10.1007/s10543-025-01058-9>.
- [36] Boyaval S. A fast Monte-Carlo method with a reduced basis of control variates applied to uncertainty propagation and Bayesian estimation. *Comput Methods Appl Mech Engrg* 2012;241–244:190–205. <http://dx.doi.org/10.1016/j.cma.2012.05.003>.
- [37] Collier N, Haji-Ali A-L, Nobile F, von Schwerin E, Tempone R. A continuation multilevel Monte Carlo algorithm. *BIT Numer Math* 2015;55(2):399–432. <http://dx.doi.org/10.1007/s10543-014-0511-3>.
- [38] Giles M. Multilevel Monte Carlo path simulation. *Oper Res* 2008;56(3):607–17. <http://dx.doi.org/10.1287/opre.1070.0496>.
- [39] Gorodetsky A, Geraci G, Eldred M, Jakeman J. A generalized approximate control variate framework for multifidelity uncertainty quantification. *J Comput Phys* 2020;408:109257. <http://dx.doi.org/10.1016/j.jcp.2020.109257>, <https://www.sciencedirect.com/science/article/pii/S0021999120300310>.
- [40] Teckentrup A, Scheichl R, Giles M, Ullmann E. Further analysis of multilevel Monte Carlo methods for elliptic PDEs with random coefficients. *Numer Math* 2013;125(3):569–600. <http://dx.doi.org/10.1007/s00211-013-0546-4>.
- [41] Peherstorfer B, Willcox K, Gunzburger M. Optimal model management for multifidelity Monte Carlo estimation. *SIAM J Sci Comput* 2016;38(5):A3163–94. <http://dx.doi.org/10.1137/15M1046472>, [arXiv:https://doi.org/10.1137/15M1046472](https://doi.org/10.1137/15M1046472).
- [42] Peherstorfer B, Willcox K, Gunzburger M. Survey of multifidelity methods in uncertainty propagation, inference, and optimization. *SIAM Rev* 2018;60(3):550–91. <http://dx.doi.org/10.1137/16M1082469>, [arXiv:https://doi.org/10.1137/16M1082469](https://doi.org/10.1137/16M1082469).
- [43] Jung W, Taflanidis AA, Kyprioti AP, Zhang J. Adaptive multi-fidelity Monte Carlo for real-time probabilistic storm surge predictions. *Reliab Eng Syst Saf* 2024;247:109994. <http://dx.doi.org/10.1016/j.res.2024.109994>.
- [44] Li Z, Montomoli F. Aleatory uncertainty quantification based on multi-fidelity deep neural networks. *Reliab Eng Syst Saf* 2024;245:109975. <http://dx.doi.org/10.1016/j.res.2024.109975>.
- [45] Shang X, Su L, Fang H, Zeng B, Zhang Z. An efficient multi-fidelity kriging surrogate model-based method for global sensitivity analysis. *Reliab Eng Syst Saf* 2023;229:108858. <http://dx.doi.org/10.1016/j.res.2022.108858>.
- [46] Croci M, Willcox KE, Wright SJ. Multi-output multilevel best linear unbiased estimators via semidefinite programming. *Comput Methods Appl Mech Engrg* 2023;413:116130. <http://dx.doi.org/10.1016/j.cma.2023.116130>.
- [47] Schaden D, Ullmann E. On multilevel best linear unbiased estimators. *SIAM/ASA J Uncertain Quantif* 2020;8(2):601–35. <http://dx.doi.org/10.1137/19M1263534>.
- [48] Geraci G, Eldred M, Iaccarino G. A multifidelity control variate approach for the multilevel Monte Carlo technique. *Cent Turbul Res Annu Res Briefs* 2015;61–71.
- [49] Fleeter CM, Geraci G, Schiavazzi DE, Kahn AM, Marsden AL. Multilevel and multifidelity uncertainty quantification for cardiovascular hemodynamics. *Comput Methods Appl Mech Engrg* 2020;365:113030. <http://dx.doi.org/10.1016/j.cma.2020.113030>, <https://www.sciencedirect.com/science/article/pii/S0045782520302140>.
- [50] Clare MCA, Leijnse TWB, McCall RT, Diermanse FLM, Cotter CJ, Piggott MD. Multilevel multifidelity Monte Carlo methods for assessing uncertainty in coastal flooding. *Nat Hazards Earth Syst Sci* 2022;22(8):2491–515. <http://dx.doi.org/10.5194/nhess-22-2491-2022>, <https://nhess.copernicus.org/articles/22/2491/2022/>.
- [51] Warne DJ, Prescott TP, Baker RE, Simpson MJ. Multifidelity multilevel Monte Carlo to accelerate approximate Bayesian parameter inference for partially observed stochastic processes. *J Comput Phys* 2022;469:111543. <http://dx.doi.org/10.1016/j.jcp.2022.111543>, <https://www.sciencedirect.com/science/article/pii/S0021999122006052>.
- [52] Nelson B. Control variate remedies. *Oper Res* 1990;38(6):974–92. <http://dx.doi.org/10.1287/opre.38.6.974>, [arXiv:https://doi.org/10.1287/opre.38.6.974](https://doi.org/10.1287/opre.38.6.974).
- [53] Pasupathy R, Schmeiser B, Taaffe M, Wang J. Control-variate estimation using estimated control means. *IIE Trans* 2012;44(5):381–5. <http://dx.doi.org/10.1080/0740817X.2011.610430>, [arXiv:https://doi.org/10.1080/0740817X.2011.610430](https://doi.org/10.1080/0740817X.2011.610430).
- [54] Mehni MB, Mehni MB. Reliability analysis with cross-entropy based adaptive Markov chain importance sampling and control variates. *Reliab Eng Syst Saf* 2023;231:109014. <http://dx.doi.org/10.1016/j.res.2022.109014>.
- [55] Ng L, Willcox K. Multifidelity approaches for optimization under uncertainty. *Internat J Numer Methods Engrg* 2014;100(10):746–72. <http://dx.doi.org/10.1002/nme.4761>.
- [56] Qian E, Peherstorfer B, O'Malley D, Vesselinov VV, Willcox K. Multifidelity Monte Carlo estimation of variance and sensitivity indices. *SIAM/ASA J Uncertain Quantif* 2018;6(2):683–706. <http://dx.doi.org/10.1137/17M1151006>.
- [57] Menhorn F, Geraci G, Seidl DT, Marzouk YM, Eldred MS, Bungartz H-J. Multilevel Monte Carlo estimators for derivative-free optimization under uncertainty. *Int J Uncertain Quantif* 2024;14(3):21–65. <http://dx.doi.org/10.1615/Int.J.UncertaintyQuantification.2023048049>.
- [58] Dixon TO, Warner JE, Bomarito GF, Gorodetsky AA. Covariance expressions for multifidelity sampling with multioutput, multistatistic estimators: Application to approximate control variates. *SIAM/ASA J Uncertain Quantif* 2024;12(3):1005–49. <http://dx.doi.org/10.1137/23M1607994>.
- [59] Zhao Y-G, Lu Z-H. *Structural reliability: approaches from perspectives of statistical moments*. Hoboken, NJ: Wiley; 2021.
- [60] Avramidis A, Wilson J. A splitting scheme for control variates. *Oper Res Lett* 2019;14(4):187–98. [http://dx.doi.org/10.1016/0167-6377\(93\)90069-S](http://dx.doi.org/10.1016/0167-6377(93)90069-S), <https://www.sciencedirect.com/science/article/pii/016763779390069S>.
- [61] Fishman G. *Monte Carlo: concepts, algorithms and applications*. New York, NY: Springer; 1996.
- [62] Valdebenito M, Jensen H, Hernández H, Mehrez L. Sensitivity estimation of failure probability applying line sampling. *Reliab Eng Syst Saf* 2018;171:99–111. <http://dx.doi.org/10.1016/j.res.2017.11.010>.
- [63] Cho S. Probabilistic analysis of seepage that considers the spatial variability of permeability for an embankment on soil foundation. *Eng Geol* 2012;133–134:30–9. <http://dx.doi.org/10.1016/j.enggeo.2012.02.013>, <https://www.sciencedirect.com/science/article/pii/S0013795212000944>.
- [64] Haftka R, Gürdal Z. *Elements of structural optimization*. third ed.. Dordrecht, The Netherlands: Kluwer; 1992.
- [65] González I, Valdebenito M, Correa J, Jensen H. Calculation of second order statistics of uncertain linear systems applying reduced order models. *Reliab Eng Syst Saf* 2019;190:106514. <http://dx.doi.org/10.1016/j.res.2019.106514>, <https://www.sciencedirect.com/science/article/pii/S0951832019301115>.
- [66] Chiron M, Genest C, Morio J, Dubreuil S. Failure probability estimation through high-dimensional elliptical distribution modeling with multiple importance sampling. *Reliab Eng Syst Saf* 2023;235:109238. <http://dx.doi.org/10.1016/j.res.2023.109238>.
- [67] Eischens R, Li T, Vogl GW, Cai Y, Qu Y. State space neural network with nonlinear physics for mechanical system modeling. *Reliab Eng Syst Saf* 2025;259:110946. <http://dx.doi.org/10.1016/j.res.2025.110946>.
- [68] Mathpati YC, More KS, Tripura T, Nayek R, Chakraborty S. MAnTRA: A framework for model agnostic reliability analysis. *Reliab Eng Syst Saf* 2023;235:109233. <http://dx.doi.org/10.1016/j.res.2023.109233>.
- [69] Yu Q, Xu J. Distribution reconstruction and reliability assessment of complex LSFs via an adaptive non-parametric density estimation method. *Reliab Eng Syst Saf* 2025;254:110609. <http://dx.doi.org/10.1016/j.res.2024.110609>.
- [70] Stokes B. mathStatica 2.5. *J Stat Softw* 2012;47(1):1–12. <http://dx.doi.org/10.18637/jss.v047.s01>, <https://www.jstatsoft.org/v047/s01>.